PLOS ONE

RESEARCH ARTICLE

Single-nuclei transcriptome analysis of channel catfish spleen provides insight into the immunome of an aquaculture-relevant species

Johanna E. Aldersey[1,2], **Miles D. Lange**[2], **Benjamin H. Beck**[2], **Jason W. Abernathy**[2]*

1 Oak Ridge Institute for Science and Education, Agricultural Research Service Research Participation Program, Oak Ridge, TN, United States of America, **2** United States Department of Agriculture, Agricultural Research Service, Aquatic Animal Health Research Unit, Auburn, AL, United States of America

* jason.abernathy@usda.gov

Citation: Aldersey JE, Lange MD, Beck BH, Abernathy JW (2024) Single-nuclei transcriptome analysis of channel catfish spleen provides insight into the immunome of an aquaculture-relevant species. PLoS ONE 19(9): e0309397. https://doi.org/10.1371/journal.pone.0309397

Editor: Md Rajib Sharker, PSTU: Patuakhali Science and Technology University, BANGLADESH

Received: June 27, 2024

Accepted: August 12, 2024

Published: September 26, 2024

Data Availability Statement: The single nuclei RNA sequencing files are available from the NCBI Gene Expression Omnibus (GEO) repository (Accession number GSE268023). All other relevant data are within the paper and its Supporting Information files.

Funding: "This research was supported by funds appropriated to the United States Department of Agriculture under Agricultural Research Service (ARS) Project #6010-32000-027-000-D to MDL, BHB, and JWA. This research was supported in

Abstract

The catfish industry is the largest sector of U.S. aquaculture production. Given its role in food production, the catfish immune response to industry-relevant pathogens has been extensively studied and has provided crucial information on innate and adaptive immune function during disease progression. To further examine the channel catfish immune system, we performed single-cell RNA sequencing on nuclei isolated from whole spleens, a major lymphoid organ in teleost fish. Libraries were prepared using the 10X Genomics Chromium X with the Next GEM Single Cell 3' reagents and sequenced on an Illumina sequencer. Each demultiplexed sample was aligned to the Coco_2.0 channel catfish reference assembly, filtered, and counted to generate feature-barcode matrices. From whole spleen samples, outputs were analyzed both individually and as an integrated dataset. The three splenic transcriptome libraries generated an average of 278,717,872 reads from a mean 8,157 cells. The integrated data included 19,613 cells, counts for 20,121 genes, with a median 665 genes/cell. Cluster analysis of all cells identified 17 clusters which were classified as erythroid, hematopoietic stem cells, B cells, T cells, myeloid cells, and endothelial cells. Subcluster analysis was carried out on the immune cell populations. Here, distinct subclusters such as immature B cells, mature B cells, plasma cells, γδ T cells, dendritic cells, and macrophages were further identified. Differential gene expression analyses allowed for the identification of the most highly expressed genes for each cluster and subcluster. This dataset is a rich cellular gene expression resource for investigation of the channel catfish and teleost splenic immunome.

Introduction

The immune system provides protection from invading pathogens and is divided into the innate immune response and the adaptive immune response. The innate immune system is a

part by an appointment (Research Fellowship to JEA) to the ARS Research Participation Program administered by the Oak Ridge Institute for Science and education (ORISE) through an interagency agreement between the U.S. Department of Energy (DOE) and the U.S. Department of Agriculture (USDA). ORISE is managed by ORAU under DOE contract number DE-SC0014664. There was no additional external funding received for this study."

Competing interests: The authors have declared that no competing interests exist.

rapid, generalized response to pathogens, whereas the adaptive immune response is a slower but targeted defense. Additionally, there are immune system agents with both innate and adaptive functions. Teleost fish are an important comparative model for the immune system given that they are lower order vertebrates with both elements of innate and adaptive immune systems [1]. The innate immune system of teleost consists of monocytes/macrophages, granulocytes, dendritic cells (DCs), natural killer (NK) cells and innate lymphoid cells (ILC) [2].

The major lymphoid organs in teleost are the thymus, head kidney and spleen [3]. Like in mammals, the thymus generates and differentiates T cells [3]. The head kidney is the fish equivalent to bone marrow in mammals [3]. The spleen provides an environment for lymphocytes, B and T cells, to exist and proliferate [4]. By maintaining these cells, the spleen also facilitates contact between the lymphocytes and antigens/antigen presenting cells to mount an immune response [4]. Furthermore, the spleen acts as a filter to clear circulating antigens and pathogens from the blood [4] and maintains erythrocyte homeostasis.

Zebrafish (*Danio rerio*) is the most studied teleost immune model. Besides zebrafish, the channel catfish (*Ictalurus punctatus*) has also served as an immunological model for the teleost innate and adaptive immune system [5]. Though compared to mammals, in particular human and mice, complex interactions of the innate and adaptive immunity are not well understood. It is evident that the main mechanisms of the immune system overlap between teleost and mammals [5,6]. However, even within teleost, there are unique attributes. For example, catfish only express IgD and IgM, while IgZ/T isotypes have been detected in zebrafish, salmonids, and other teleost fish [7–10].

The production of channel and hybrid catfish are of great commercial interest as they represent the largest sector of the United States (U.S.) aquaculture industry, with sales generating $437 million in 2023 [11]. Significant losses in production can be attributed to pathogenic diseases, and epidemiological reports show that catfish production is most affected by bacterial diseases such as motile *Aeromonas* septicemia caused by *Aeromonas hydrophila*, columnaris disease caused by *Flavobacterium covae* and enteric septicemia caused by *Edwardsiella ictaluri* [12]. A basic understanding of the catfish adaptive immune system will facilitate investigation into the progression of aquaculture-relevant diseases. Furthermore, the single-nuclei data produced from this study will be used to provide a baseline for studying the effects of active infection and disease interventions such as vaccines.

Studying the immune cell types in catfish and their gene expression profiles has been limited to bulk RNA sequencing (RNAseq) [13–15]. Bulk RNAseq extracts transcriptomic information from a tissue or cell population, and thus the data represents the average gene expression of the cells [16]. Therefore, for samples with heterogenous cell populations, transcriptomic information is mixed, and signals from rare cell types are obscured or not detected [16]. However, the additional characterization of immune cells in the heterogenous lymphoid tissues is now possible with single-cell/single-nuclei RNAseq (scRNAseq/snRNAseq). In sc- and snRNAseq, the transcriptomic analysis occurs at the individual cell level, allowing cell types and states to be studied, and between cell type differences to be characterized [16]. Such technology has already been applied to study zebrafish and Atlantic salmon (*Salmo salar*) spleen to identify different immune cells [17]. To better understand the cellular landscape of the catfish spleen we generated a snRNAseq atlas for the channel catfish. The spleen atlas provides a profile for the various immune cell types in the spleen and can be used to study the expression of immune-relevant gene families.

Materials and methods

Tissue preparation

This study was carried out at the United States Department of Agriculture–Agricultural Research Service (USDA-ARS) Aquatic Animal Health Research Unit (AAHRU) and the use of fish in this study was approved by the Institutional Animal Care and Use Committee (IACUC) to ensure ethical use of research animals. The protocol conformed to USDA-ARS Policies and Procedures 130.4 and 635.1. Three channel catfish (~ 1 kg) were obtained from an earthen production pond and euthanized in a solution of MS-222 (300 mg/L, Syndel USA, Ferndale, WA) buffered with sodium bicarbonate for 10 min. The individual spleens were removed and placed into Petri dishes containing channel catfish media (cL-15), which is made of Leibovitz's L-15 medium (ThermoFisher Scientific, Waltham, MA) adjusted to catfish tonicity with PenStrep glutamine solution (ThermoFisher Scientific) and 5% FBS (R&D, Minneapolis, MN) [18]. The spleens were first processed through a 70 μM cell sieve into Petri dishes (ThermoFisher Scientific) to achieve a single cell suspension and then further processed through a 40 μM cell sieve (ThermoFisher Scientific) into 50 mL Falcon tubes and cL-15 was added up to 10 mL. The splenic cell suspensions were centrifuged at 350 x g for 5 min, the supernatant was aspirated, and the cell pellet was resuspended in 10 mL of cL-15. This process was repeated two additional times, and the final cell pellet was resuspended in 15 mL of cL-15. Splenic cells were counted, and cell viability was assessed with Trypan blue using a TC-20 cell counter (BioRad, Hercules, CA). Whole, unfractionated spleen preparations from each of the three individuals (1.0×10^7 cells) were pelleted and resuspended in 1 mL of freezing medium (90% FBS, 10% DMSO) in 2 mL CRYO.S cryogenic vials (Greiner Bio-One, Monroe, NC) and placed into a Mr. Frosty freezing container (ThermoFisher Scientific) at -80˚C for 24 h. The cryogenic vials were then moved into liquid nitrogen storage until shipping to a service provider.

Cell preparation to isolate individual nuclei

The following procedures (isolation of nuclei through the generation of raw sequencing data) were performed via a service provider (SeqMatic, Fremont, CA). Frozen cells were thawed in a water bath set to 28˚C and added to 6 mL of cL-15. The cells were centrifuged at 1200 RPM for 5 min to form a pellet. The supernatant was removed, and the cells were resuspended with 1 mL of cL-15. Cell concentrations and viability were measured using a Countess II FL automated cell counter (ThermoFisher Scientific). A total of 2.5×10^6 cells were transferred to new tubes and centrifuged at 300 x g for 5 min at 4˚C, and the supernatant was removed. The cells were lysed by gently pipette mixing in 200 μL of lysis buffer and incubated for 1 min on ice. The lysis buffer consisted of 10 mM Tris-HCL (pH 7.4), 10 mM NaCl, and 3 mM $MgCl_2$ (Millipore-Sigma, Burlington, MA).

The lysed cells were initially washed by pipette mixing with 800 μL of Nuclei Wash and Resuspension Buffer and centrifuged. The buffer contained 1% BSA (ThermoFisher Scientific), 0.2 U/μL RNase Inhibitor (Millipore-Sigma), and 1x PBS (Corning-Cellgro). The nuclei were washed two times using 1 mL of Nuclei Wash and Resuspension Buffer, pelleted by centrifugation and the supernatant removed. Centrifugation for washing steps were carried out at 500 x g for 10 min at 4˚C.

The quality of the nuclei was checked by resuspending with 100 μL of Nuclei Wash and Resuspension Buffer with Ethidium Homodimer-1 dye (Millipore-Sigma). The nuclei concentration was diluted to the target concentration required for library preparation.

Library construction

The single-nuclei RNA-seq libraries were prepared and constructed using the Chromium X Instrument (10x Genomics, Pleasanton, CA) and the Chromium Next GEM Single Cell 3' GEM Kit v3.1 (10x Genomics) following the manufacturer's protocol. Briefly, the individual nuclei were partitioned to produce gel beads-in-emulsion (GEMs). The GEMs were generated by loading the nuclei in master mix, barcoded Single Cell 3' v3.1 Gel Beads, and partitioning oil onto Chromium Next GEM Chip G. The Gel Beads was dissolved to release the primers and incubated to produce barcoded full-length cDNA. The cDNA was cleaned to removed left over reagents using Dynabeads MyOne SILANE (ThermoFisher), then amplified via PCR. Optimal sized cDNA amplicons were selected using SPRIselect (Beckman Coulter, Brea, CA) and Illumina indexes and adapters were added via end repair, A-tailing, adaptor ligation, and PCR. Sample quality was checked using a TapeStation (Agilent Technologies, Santa Clara, CA) with the TapeStation High Sensitivity D1000 ScreenTape (Agilent Technologies). The three cDNA samples were multiplexed and sequenced using the Illumina NovaSeq X Plus sequencer (San Diego, CA). The raw sequencing data was demultiplexed using Cell Ranger (v.5.0.0) 'cellranger mkfastq'and data provided to the USDA-ARS-AAHRU.

Data demultiplexing, trimming, filtering and normalization

Prior to snRNAseq data analyses, annotation of the channel catfish reference genome assembly (Coco_2.0, NCBI Accession number GCF_001660625.3) was manually curated. The annotation for IgM (ighm) was missing from the reference genome, and IgD (ighd) was annotated to include *ighm*. The reference genome annotation file (GCF_001660625.3_Coco_2.0_genomic.gtf) was adjusted to include an annotation for *ighm* (chr2:17077000–17085528) based on the channel catfish genomic DNA sequence of the IgM heavy chain (NCBI Accession number X52617.1), including four exons encoding CH1-4 and two exons encoding the transmembrane (TM) domains [19,20]. The annotation for *ighd* (NCBI Accession number XM_053677651.1) had exons (exon 1 and exon 2) that did not correspond with constant domains 1–7 or TM domains (NCBI Accession number AF363448) [10], and exon 2 overlapped with the *ighm* CH1 domain. Therefore, *ighd* was altered to the range chr2:17085529–17097451 and exon 1 and exon 2 removed.

A Cell Ranger compatible channel catfish reference genome was built using the reference assembly with the modified GTF file using 'cellranger mkref'. Sequences were trimmed, aligned to the reference assembly, filtered, and counted to generate feature-barcode matrices.

The individual spleen samples were filtered further and normalized using Seurat (v.5.0.1) [21]. Cells with number of expressed genes < 200 and $> 4{,}000$, and cells that had expression from mitochondrial genes $> 5\%$ were removed from the data. The data was normalized using the global-scaling normalization method, whereby feature expression for each cell is normalized by the total expression, multiplied by 10,000 and log transformed.

Cluster analysis

The dimensionality of the data was analyzed by principal component analysis (PCA). Prior to PCA, the expression data was scaled so that the mean expression across cells was 0, and the variance was 1. An elbow plot of the PCA standard deviations and observation of genes in PCAs was used to determine the number of dimensions used to generate clusters.

Cluster analysis was carried out on individual samples and on integrated (aggregated) samples. Samples were integrated using the 'merge', 'integrate'and 'join'functions in Seurat. Clusters were generated through a graph-based approach using the 'FindNeighbors'and 'FindClusters'functions in Seurat. Briefly, a K-nearest neighbor (KNN) graphing approach

identified cells with similar gene expression patterns, and the Louvain algorithm was applied to identify clusters. The clusters were labelled as erythroid, hematopoietic stem cells (HSC), B cells, T/NK cells, myeloid-derived cells or endothelial cells depending on gene marker expression. Markers used to define cell type were obtained from the current literature. Differential gene expression analysis was carried out between clusters using 'FindAllMarkers'.

Cell trajectory analysis

The trajectory analysis was conducted using Monocle 3 (v1.3.7) [22]. The Seurat object containing cluster information was converted to a cell data set object using SeuratWrappers (v0.3.5). The function 'learn_graph'was used to predict the trajectory, and 'order_cells'was used to determine the pseudotime of each cell. The trajectory and pseudotime were plotted onto the UMAP of clusters.

Results and discussion

Data quality

The snRNAseq libraries of each spleen from three individual channel catfish were termed SP1, SP2, and SP3. The summary statistics of the splenic snRNAseq transcriptome libraries, before filtering, generated an average of 278,717,872 reads from a mean 8,157 cells (Table 1). Filtering was carried out to remove cells likely to be non-viable, identified by higher mitochondrial DNA counts (> 5%), and from cells likely to be doublet/multiplet indicated by high molecule/feature counts. After filtering, 81.4%, 69.6% and 84.0% of cells remained for SP1, SP2, and SP3, respectively.

The individual cluster analyses identified 11 to 12 clusters for SP1, SP2, and SP3, which are numbered sequentially in order of cell number in each cluster per individual (Fig 1). The numbering does not necessarily indicate that clusters with the identical numbering between samples are the same cell type. The ten most differentially expressed gene markers were identified for individual clusters (S1 Table). Cell clusters for each library were defined when a similar number of clusters, and cluster-size distribution were identified, and an initial cell identification was proposed based on the expression of canonical genes from known cell types (Fig 1 and S1 Table). To identify cell types within the spleen libraries, genes identified from single-

Table 1. Summary statistics of single-nuclei transcriptome libraries (SP1, SP2, SP3) generated from catfish spleens (n = 3). The data were initially filtered to remove barcodes not associated with cells using Cell Ranger and further filtering was carried out using Seurat to remove multiplets and cells with > 5% reads aligned to mitochondrial genes. The individual libraries were integrated for combined cluster analysis in Seurat.

Sample	Output	SP1	SP2	SP3	Seurat Integrated Samples
Number of Reads	Cell Ranger [a]	198,304,083	215,231,958	422,617,575	
Median Number of Reads/Cell	Cell Ranger [a]	25,591	42,037	36,423	
Q30 Bases in RNA Reads	Cell Ranger [a]	95.0%	93.6%	95.2%	
Confident Alignment to Reference Transcriptome	Cell Ranger [a]	48.4%	47.7%	42.1%	
Estimated Number of Cells	Cell Ranger [a]	7,749	5,120	11,603	
	Seurat [b]	6,305	3,564	9,744	19,613
Number of Features Detected	Cell Ranger [a]	25,591	22,692	23,1456	
	Seurat [b]	19,094	19,224	20,121	20,121
Median Number of Features/Cell	Cell Ranger [a]	647	554	733	
	Seurat [b]	649	532	737	665

[a] The data were initially filtered to remove barcodes not associated with cells using Cell Ranger.

[b] The data after filtering using Seurat.

https://doi.org/10.1371/journal.pone.0309397.t001

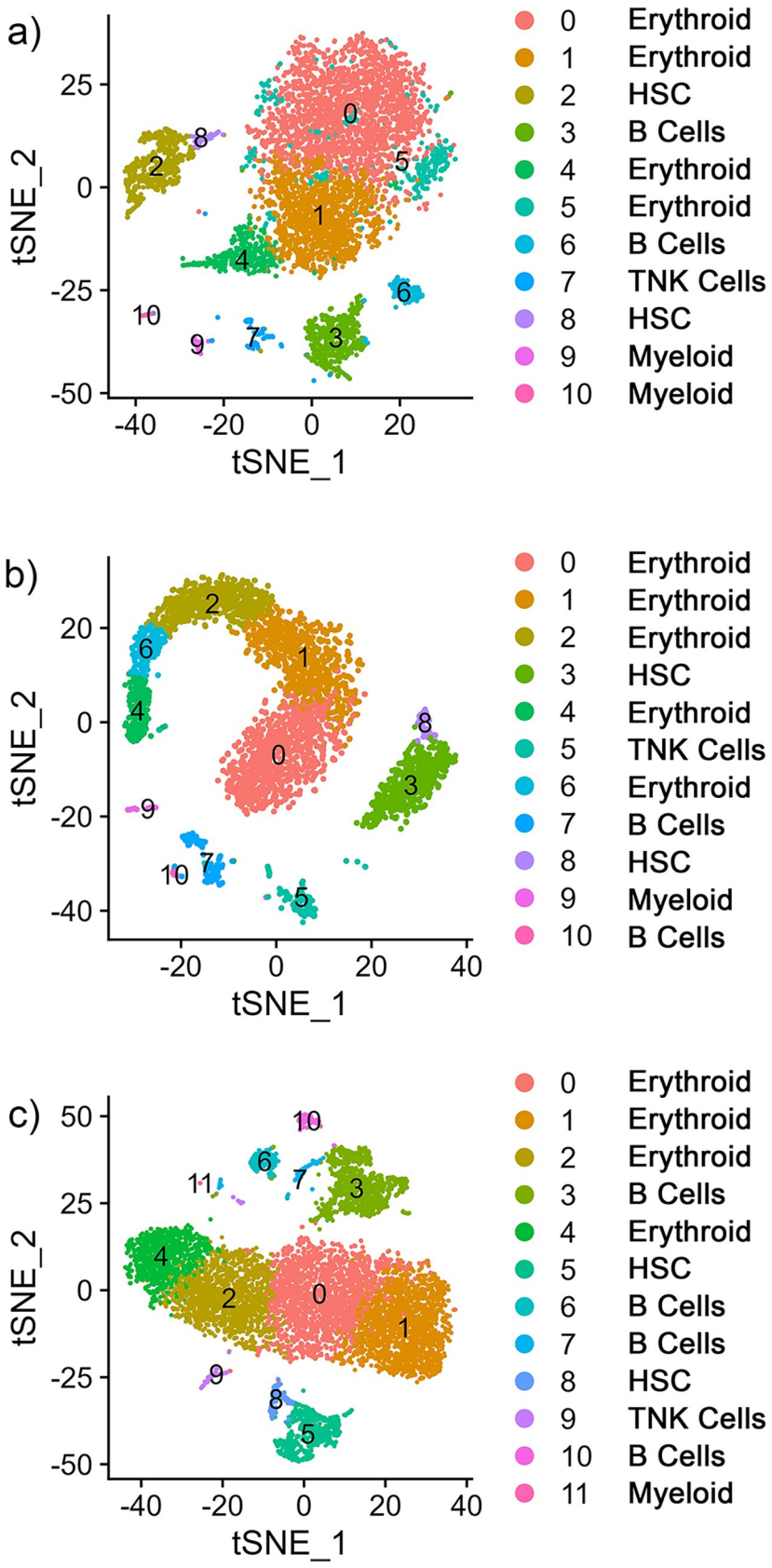
a)
tSNE_2
tSNE_1
25
0
-25
-50
-40
-20
0
20
0 Erythroid
1 Erythroid
2 HSC
3 B Cells
4 Erythroid
5 Erythroid
6 B Cells
7 TNK Cells
8 HSC
9 Myeloid
10 Myeloid
b)
tSNE_2
tSNE_1
20
0
-20
-40
-20
0
20
40
0 Erythroid
1 Erythroid
2 Erythroid
3 HSC
4 Erythroid
5 TNK Cells
6 Erythroid
7 B Cells
8 HSC
9 Myeloid
10 B Cells
c)
tSNE_2
tSNE_1
50
25
0
-25
-50
-40
-20
0
20
40
0 Erythroid
1 Erythroid
2 Erythroid
3 B Cells
4 Erythroid
5 HSC
6 B Cells
7 B Cells
8 HSC
9 TNK Cells
10 B Cells
11 Myeloid

Fig 1. Single-nuclei transcriptomes of whole spleen samples from channel catfish (*Ictalurus punctatus*). Cluster analysis was performed on individual samples (a) SP1 (b) SP2 (c) SP3. Clusters are depicted as tSNE plots and cell-markers are used to classify clusters as erythroid cells, HSC, B cells, T/NK cells, and myeloid lineage cells.

https://doi.org/10.1371/journal.pone.0309397.g001

cell analyses of different vertebrate species (mammalian and teleost) were used as a reference (Table 2). Ultimately, the individual sample libraries were integrated into one dataset for cluster analysis and cell type identification. Except for one cluster, cells from all three samples contributed to the clusters in the integrated single-cell data set (S1 Fig).

Cell populations in the channel catfish spleen

Cluster analysis of the aggregated spleen library yielded 17 clusters which were defined in the tSNE (Fig 2A) and heat map (S2 Fig). Expression of 25 canonical gene markers defined these different clusters (Fig 2B and Table 2). The majority of identified cells (14,353; 73.0%), consisting of six clusters, expressed erythroid markers. The immune cell markers further defined hematopoietic stem cells (HSC, 2,065; 10.5%), B cells (2,469; 12.5%), T/Natural Killer (NK) cells (461; 2.35%) and myeloid lineage cells (234; 1.19%). Thirty-one cells expressing endothelial markers were also identified (S2 Table and S2 Fig).

The six erythroid clusters 0–3 and 6–7 had increased expression of *slc4a1a*, *alas2*, *sptb* and *hemgn*, and uniformly grouped together (Fig 2 and S2 Table). Cluster 0 had significantly increased expression of blood related genes *LOC108257039* (hemoglobin subunit beta), *blvrb* (biliverdin reductase B), *hbaa2* (hemoglobin subunit alpha 2), *mt2* (metallothionein 2), and *urod* (uroporphyrinogen decarboxylase). In humans, *MT2A* is a negative regulator of erythroid differentiation [33]. The human orthologue of *blvrb* maintains redox homeostasis and is involved in directing cell fate of HSC to red blood cells [34]. The gene *urod* encodes an enzyme involved in heme production [35]. Cluster 1 has significantly increased expression of *pcmt* (protein-L-isoaspartate O-methyltransferase) which is involved in repair of red blood cells undergoing oxidative stress in mice [36]. Therefore, this cluster may represent red blood cells with oxidative stress. Cluster 2 cells significantly increased expression of hemoglobin subunits, *LOC108257036* (hemoglobin subunit beta) and *LOC108257041* (hemoglobin subunit alpha). The remaining genes highly expressed by this cluster have not been characterized. Cluster 3 cells have increased expression of *ank1a* (ankyrin 1), *sox6* (SRY-box transcription factor 6), *LOC108280488* (transferrin receptor), *ripor3*, *slc7a5* (Solute carrier family 7 member 5). Ankyrin is a protein that attaches to the cell membrane to maintain the membrane structure of erythrocytes [37]. *Sox6* is involved in erythroid maturation [38]. Human and murine orthologues of *slc7a5* control red blood cell size and maturation and absent in mature erythroid cells [39]. Therefore, Cluster 3 cells may represent immature erythroid cells. Cells in cluster Erythroid 6 was defined only by increased ribosomal protein expression. Cluster 7 had increased

Table 2. Features used to identify each cell type among different clusters.

Population	Feature	Reference
Erythroid cells	*slc4a1a*, *alas2*, *sptb*, *hemgn*	[6,23,24]
B cells	*pax5*, *cd79b*, *cd37*, *ighd*, *ighm*	[6,25]
T/NK cells	*lck*, *runx3*, *ifgn1*, *il7r*	[6,26,27]
HSC	*meis1b*, *mpl*, *runx1*, *gata2b*	[6,28–30]
Myeloid cells	*adgrg3*, *nccrp1*, *mpeg1.1*, *grna*	[6,31]
Endothelial cells	*cdh5*, *kdrl*, *pecam1a*, *akap12b*	[6,32]

https://doi.org/10.1371/journal.pone.0309397.t002

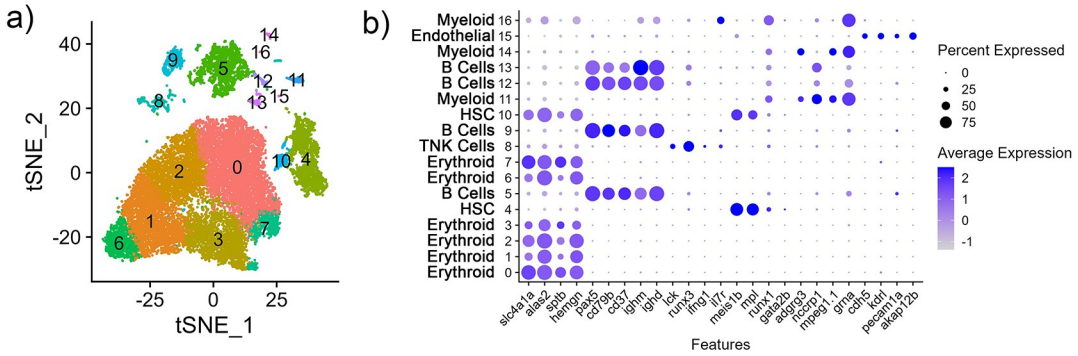

Fig 2. Cluster analysis of integrated nuclei transcriptome of spleen (n = 3) from channel catfish. Cluster analysis identified sixteen cell clusters. (a) tSNE plot (b) Average expression (z-score) of cell type markers (x-axis) for each cluster (y-axis). The size of the dot represents the percentage of cells per cluster contributing to expression. Cell type was assigned to clusters based on the expression of canonical cell markers (Table 2).

https://doi.org/10.1371/journal.pone.0309397.g002

expression of *slc4a1a*, *LOC108280488* (transferrin receptor), *ripor3*, *ank1a*, *sptb*, *blvrb* and *epb41b* (erythrocyte membrane protein band 4.1b).

Cluster 4 had increased expression of *itga2b* (integrin alpha 2b; also known as *cd41*), *meis1b* (meis homeobox 1) and *itgb3b* (integrin beta 3b; also known as *cd61*) which are genes known to be expressed by HSC (Table 2). *Itga2b/itgb3b* are used as a marker for HSC in teleost fish [40,41] and other species [42–44]. The expression of the transcription factor *meis1b* has been detected in HSC isolated from zebrafish kidney [45], and was shown to be important for the maintenance of adult mouse HSC [46]. Cluster 10 (HSC) expressed both erythroid (*slca1a*, *alas2*, *sptb*, *hemgn*) and HSC markers (*meis1b*, *mpl*, *runx1*).

There are four clusters (Clusters 5, 9,12–13) that have expressed B cell markers *pax5*, *ighd*, *ighm*, *cd79b* and *cd37* (Fig 2B and S2 Table). Clusters 5 and 9 have *pax5*, *ighd*, *LOC108259908* and *nr4a1* (nuclear receptor subfamily 4 group A member 1) among their most highly expressed genes. *LOC108259908* is assigned to an Ig heavy chain Mem5-like gene in the current channel catfish genome assembly (Coco_2.0), but likely represents an IgL gene segment based on BLAST analysis [47,48]. *Pax5* and *ighd* are canonical B cell genes [49,50] and *nr4a1* is expressed in a wide variety of immune cells, including macrophages, but, in mice, functions to restrain immunodominance of B and T cells when diverse clonal population compete in the germinal center (GC) [51,52]. In the apparent absence of GC in teleost fish perhaps it is more important in regulating the formation or maintenance of melano-macrophage centers [53,54]. Cluster 5 also had increased expression of *ebf1b* (early B cell transcription factor 1b), *LOC108261469* (immunoglobulin kappa constant-like) and *pou2af1* (POU class 2 homeobox associating factor 1). In teleost, *ebf1b* is expressed by the common lymphoid progenitor, pro-B cells and pre-B cells and drives early B cell commitment [49]. This suggests that the cells in Cluster 5 could represent a nascent B cell lineage. Cluster 9 also had increased expression of *LOC108267808* (LYN proto-oncogene) and *cd79b*. Expression of *LYN* and *cd79* have been shown to be important for B cell receptor formation, maturation, and survival [55,56].

The remaining B cell clusters, 12 and 13, have higher expression of *fabp3* (fatty acid binding protein 3) and *mki67* (marker of proliferation Ki-67). In mice, *fabp3* is expressed in activated B cells and promotes the development of plasma cells [57]. *MKI67* expression was increased in human bone marrow plasmablasts [58]. The expression of *fabp3* and *mki67* indicates that these cells may have differentiated from B cells to plasmablasts. The cells in Cluster 12 also have increased expression of *diaph3* (diaphanous-related formin 3) and *atp5mc1* (ATP

synthase membrane subunit c locus 1). The human orthologues of *diaph3* and *atp5mc1* are expressed by human plasma cells [59]. The cells in Cluster 13 have increased expression of *pdia4* (protein disulfide isomerase family A, member 4), *selenom* (selenoprotein M), *spats2* (spermatogenesis associated serine rich 2), *hsp90b1* (heat shock protein 90 beta family member 1), *stt3a* (STT3 oligosaccharyltransferase complex catalytic subunit A), *ube2j1* (ubiquitin conjugating enzyme E2 J1), and *lman1* (Lectin, mannose binding 1). In mice, it has been shown that *hsp90b1* acts as a chaperone to toll-like receptors and integrin molecules [60]. The human single cell type atlas indicates that *PDIA4*, *SELENOM*, *SPATS2*, *HSP90B1*, *STT3*, *UBE2J1* and *LMAN1* are expressed by human plasma cells [59].

Cluster 8 expressed T cell markers *lck*, *runx3*, *ifng1* and *il7r* (Fig 2B and S2 Table). The most differentially expressed genes indicative of T cell function include *ptprc* (protein tyrosine phosphatase receptor type C), *runx3*, *fmnl1a* (formin like 1) and *arid5a* (AT-rich interaction domain 5A). *Ptprc* is expressed by most immune cells but is important for T cell development and signaling, and NK cell function [61–63]. *Runx3* is a transcription factor for T cell development [64]. In mice, *fmnl* was shown to be important for T cell migration through restrictive environments [65]. *Arid5a* directs differentiation of naive $CD4^+$ T cells to inflammatory $CD4^+$ T cells [66].

Clusters 11, 14 and 16 have increased expression of *adgrg3*, *nccrp1*, *mpeg1.1* and *grna* indicating that they likely belong to the common myeloid cell lineage (Fig 2B). Cluster 11 was defined by upregulated expression of myeloid-related genes such as *dbn1* (drebrin 1), *foxp4* (forkhead box P4), *samsn1a* (SAM domain, SH3 domain and nuclear localization signals 1), *csf1rb* (colony stimulating factor 1 receptor), *mafba* (MAF bZIP transcription factor B) and *csf3r* (colony stimulating factor 3 receptor). *Dbn1* is expressed by DCs and mast cells in mice and encodes drebrin which is an actin binding and stabilizing protein [67,68]. An *in vitro* study of *FOXP4* has shown that it may have a role in the inflammatory response of human neutrophils [69]. The *samsn1* mouse orthologue regulates inflammatory response of immune cells, including macrophages, mast cells and lymphoid cells [70]. In humans, *MAFB*, a transcription factor, is involved in cell fate of myeloid cells which can differentiate to either macrophages and DCs [71]. Lastly, *csf1r* encodes a receptor that regulates monocytes and macrophages in teleost species [72], and was demonstrated to promote the differentiation of myeloid progenitors into leukocytes such as monocytes, macrophages and DCs in human and mouse studies [73]. *LOC108266645* (killer cell lectin-like receptor subfamily E member 1) is also highly expressed and may indicate pre-cursors to DCs are present in this group. Killer cell lectin-like receptors typically modulate DC and NK cell immune responses [74,75].

Cluster 14 had increased expression of myeloid-lineage genes *flt3* (fms related receptor tyrosine kinase 3), *fgd4a* (FYVE, RhoGEF and PH domain containing 4a), *plxna4* (plexin A4), *dbn1*, *ppfibp2* (ppfibp2a), *pak1* (P21 (RAC1) activated kinase 1). *Flt3* is involved in differentiation of myeloid progenitors into macrophages (mouse) and DCs [76,77]. The *pak1* mouse orthologue was shown to be involved with macrophage polarization [78]. Human orthologues of *fgd4a* and *ppfibp2* have expression in monocytes, and *plxna4* has expression in DCs. Myeloid related genes that were upregulated in Cluster 16 were *apol1* (apolipoprotein L1), *sting1* (stimulator of interferon response cGAMP interactor 1), *LOC108279184* (transcription factor 4; *tcf4*), *LOC108266986* (TLR adaptor interacting with endolysosomal SLC15A4), *nitr6* (novel immune-type receptor 6) and *ctss1* (cathepsin S). There is some evidence that human *apol1* orthologues may be involved with DC cell death [79]. *Sting1* is a well-characterized transmembrane protein of the endoplasmic reticulum involved in inflammation and immune response to pathogens by producing type 1 interferons and pro-inflammatory cytokines [80]. Human *STING1* expression is detected in diverse immune cells, including macrophages, T cells and NK cells [59]. The human orthologue of *LOC108266986*, *TASL*, is involved in immune

responses through the production of cytokines and chemokines, primarily in plasma cells, DCs and macrophages [81]. The human orthologue of *LOC108279184*, *TCF4*, has been shown to be expressed by human DCs [59] and important for plasmacytoid DC development [82]. *Nitr* family genes were first identified in pufferfish and do not have a human orthologue [83]. This family of genes are predicted to have similar functions to leukocyte receptor complex genes [84]. *Ctss1* encodes cathepsin S and reported to be expressed by macrophages, B cells and dendritic cells [85]. In *I. punctatus*, cathepsin S genes were upregulated in mucosal surfaces in response to bacterial infection [85].

Cluster 15 expressed endothelial marker genes *cdh5*, *kdrl*, *pecam1a*, *akap12b*, *znf521*, *calcrl*. These cells are most often associated with vascular and lymphatic development [86,87].

Characterization of the immunome

To gain additional insight into the splenic immunome, the erythroid cells (Fig 2) were filtered from the integrated data and cluster analysis was again performed on the remaining 5,269 cells. This analysis identified 15 immune cell clusters (S3 and S4 Figs and S3 Table).

Additional subclusters have been defined for HSC, B cells, T cells and myeloid cells. The archetype markers (Table 2) were used to validate the subcluster cell types and differential expression analysis identified the unique expression patterns of each subcluster.

HSC cells were further defined into 4 subclusters, HSC0 (932 cells), HSC1 (483 cells), HSC2 (371 cells), HSC3 (279 cells) using the top differentially expressed genes (Figs 3A and S5, S4 Table). HSC0-2 seemed consistent in their expression of known HSC genes (Fig 3B–3L) [40,41]. HSC3 however had much less expression of these genes and an increased expression of genes often associated with erythroid-cell function such as *alas2* (5'-aminolevulinate synthase 2), *hbb* (hemoglobin subunit beta), *slc4a1a* (solute carrier family 4 member 1), and *LOC108257040* (hemoglobin subunit alpha) (S4 Table). This cluster also had increased expression of the erythroid markers *sptb* and *hemgn*. One hypothesis is that the HSC that express erythroid markers are erythroid progenitors. Hematopoietic stem and progenitor cells with erythroid marker expression have also been identified in the zebrafish spleen [6]. The authors suggested that these cells were potentially erythroid progenitors. Another hypothesis is that the erythroid markers represent partially differentiated cells that can develop into multiple cell lineages. The erythroid markers were common between three subclusters of cells for HSC, B cells, and T cells. Thus, since HSC differentiates to lymphocytes, the cells could be progenitors. A third hypothesis is that the erythroid-like cells are erythrocytes with immune functions. There is evidence of erythrocytes expressing some immune genes. In the case of Nile tilapia (*Oreochromis niloticus*), erythrocytes expressed interferon regulatory factors that were also expressed by leukocytes [88]. However, our data shows that the channel catfish erythroid-like cells have similarities with lymphocytes. Additional investigation is required to further elucidate the classification of these cell subtypes.

Further examination of 2,469 splenic B cells identified 9 subclusters, B0-B8 (Fig 4A), wherein these subclusters have expressed the canonical B cell markers and further been defined using the top differentially expressed genes (Figs 4B and S6, S5 Table). Based on their gene expression we sought to identify different B cell lineage developmental stages [89,90]. In subcluster B1 (489 cells), *zeb2b* was most significantly expressed and in subcluster B4 (201 cells), *ebf1b* was the most significant (S5 Table). Subclusters B1 and B4 also both had higher expression of *ikzf1* and *foxp1b* relative to the remaining cluster cells (Figs 4B and S7). These genes are well defined transcription factors required for early B cell differentiation [91,92]. Subcluster B1 also had significantly highly expressed *ets1*, another known B cell development regulator [93]. Taken together these results suggest that B1 and B4 likely represent an

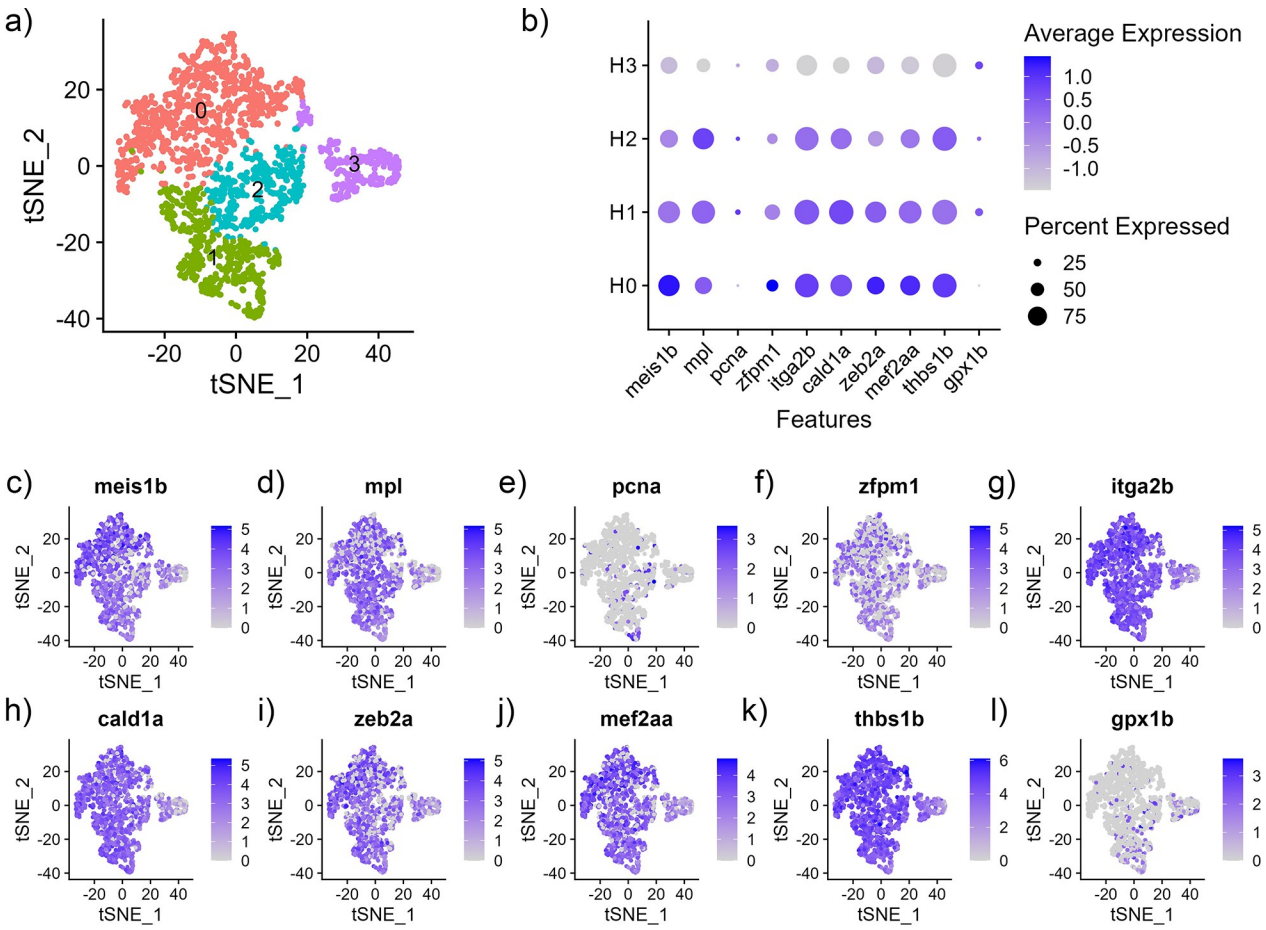

Fig 3. Subcluster analysis of hematopoietic (HSC) cells from the integrated nuclei transcriptome of spleen from channel catfish. (a) tSNE plot (b) Average expression (z-score) of cell type markers (x-axis) for each cluster (y-axis). The size of the dot represents the percentage of cells per cluster contributing to expression. (c-l) Feature maps of HSC gene expression on tSNE plots.

https://doi.org/10.1371/journal.pone.0309397.g003

immature stage of B cell development in the spleen. In contrast, subclusters B2 (343 cells), B3 (288 cells) and B7 (124 cells) relative to the remaining clusters had higher expression of *il6r* and *cd40*, cell surface receptors, and *mycb*, a transcription factor [94,95]. B3 also had higher expression of *cxcr4b* and the analysis of the most differentially expressed genes identified *LOC108280570* (*homer3*) and *ccr9a* expression (S5 Table). Therefore, B2, B3 and B7 likely represent varying mature B cell populations. Lastly, subclusters B6 (125 cells) and B8 (103 cells) have higher expression of genes associated with plasmablasts and plasma cells (Fig 4B). B6 has greater expression of *selenom* and *irf4l* (S5 Table), and relative to the other clusters had higher expression of *ighm*, *prdm1a* and *xbp1* (Figs 4B and S7) [96–98]. B8 had significantly greater expression of *mki67* and *top2a* (S5 Table) and relative to some clusters had less expression of *pax5* (Figs 4B and S7).

Cluster analysis using 461 splenic T/NK cells identified 6 subclusters which have expressed canonical T and NK cell markers and were further defined using the top differentially expressed genes (Fig 5A, S6 Table and S8 Fig). Interestingly, except for a few cells, the T cells did not express *cd4* (*cd4-1*, *cd4-2.2*) or *cd8* (*cd8a*, *cd8b*) genes (S9 Fig) suggesting that these cells are not differentiated as helper T cells or cytotoxic T cells. Subcluster T0 (127 cells) most significantly expressed *tcf7*, *LOC108256553* (DNA-binding protein SATB1), and *rgs3a*

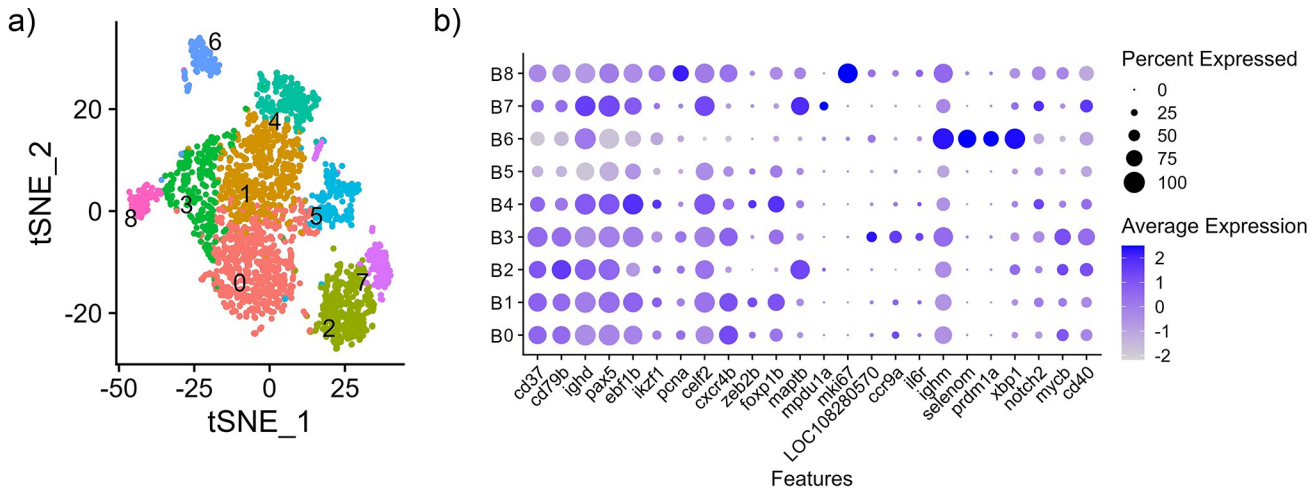

Fig 4. Subcluster analysis of B cells from the integrated nuclei transcriptome of spleen from channel catfish. (a) tSNE plot (b) Average expression (z-score) of cell type markers (x-axis) for each cluster (y-axis). The size of the dot represents the percentage of cells per cluster contributing to expression.

https://doi.org/10.1371/journal.pone.0309397.g004

(regulator of G protein signaling 3a) (Fig 5B and S6 Table), which facilitate differentiation and regulation of T cell function [99,100]. T0 also had significantly increased expression of *tox* (thymocyte selection-associated high mobility group box) and *tox2* (TOX high mobility group box family member 2) that also contribute to the functional maintenance of T cells and NK cells (S9 Fig and S6 Table) [101–107]. T0 also has significantly expressed transcription factors *LOC128635459* (*znf239*) and *znf704*, which also likely have a role in lymphocyte development and are representative of naïve T cells [108]. Subcluster T1 (91 cells) has significantly increased expression of several genes that make up the T cell receptor complex (TCR). These genes include gamma (*LOC108267226*, *LOC108267144*), delta (*LOC108267350*), and *cd247* TCR genes (Fig 5B and S6 Table) [109,110]. T1 also had increased expression of *LOC108264986* (tyrosine-protein kinase ZAP-70*)*, a gene that encodes a tyrosine kinase involved in the proximal TCR signaling and T cell activation [111], *mafa* (MAF bZIP transcription factor), which is a transcription factor that regulates T cell specification and maintenance [112] and *bcl11ba*, a

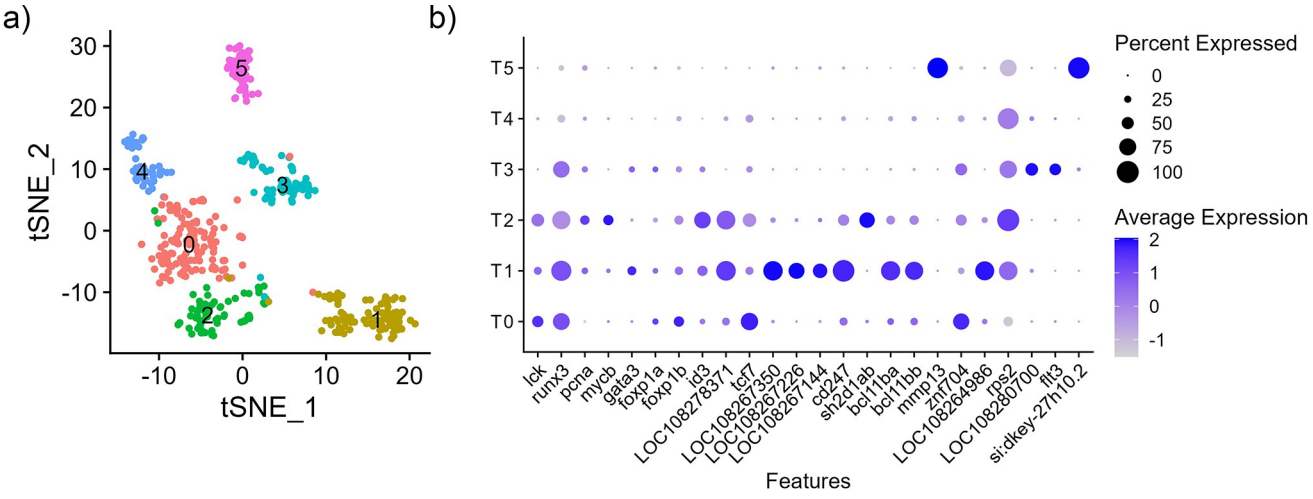

Fig 5. Subcluster analysis of T/NK cells from integrated nuclei transcriptome of spleen from channel catfish. (a) tSNE plot (b) Average expression (z-score) of cell type markers (x-axis) for each cluster (y-axis). The size of the dot represents the percentage of cells per cluster contributing to expression.

https://doi.org/10.1371/journal.pone.0309397.g005

zinc finger transcription factor that is critical for T cell maintenance and identity [113]. Subcluster T1 expression seems to be consistent with that of γδ T cells; however, they are not often associated with primary lymphoid tissues in vertebrates [114,115]. Subcluster T2 (72 cells) had significant expression of *sh2d1a* (SH2 domain containing 1A), *hcst* (hematopoietic cell signal transducer; also known as *DAP10*), *gzmb3.3* (granzyme B) and *gzmk* (granzyme K), that have functional pathways in both T and NK cells (Figs 5B and S9, S6 Table) [116–119]. T2, relative to the other subclusters, also had higher expression of *id3* and *LOC1082788371* (*CD3ε*) (Fig 5B) which, taken together, would likely classify these as effector T cells [120]. Subcluster T3 (65 cells) had increased expression of genes that encode receptors and membrane bound proteins found expressed among different immune cell types, thus, the cells may represent innate-like lymphoid cells (ILC). T3 subcluster genes, *flt3* (fms related receptor tyrosine kinase 1), *LOC108266645* (killer cell lectin-like receptor subfamily E member 1), *prf1* (perforin 1) and *pag1* (phosphoprotein membrane anchor with glycosphingolipid microdomains 1) represent functional pathways in DC, NK and T cell phenotypes. In addition, *zeb2b* (zinc finger E-box binding homeobox 2) also has non-specific immune cell expression [59]. Subcluster T4 is characterized by greater expression of erythroid genes, including *LOC108257039* (hemoglobin cathodic subunit beta), *alas2*, *LOC108268628* (calpain8), *gpx1a*, *blvrb*, *hba*, and *cahz*. Interestingly, subcluster T5 (53 cells) had increased expression of myeloid markers. Four of the top ten differentially expressed genes, *mmp13* (matrix metallopeptidase 13), *mmp9* (matrix metallopeptidase 9), *ms4a4a* (membrane spanning 4-domains A4A) and *gpr84* (G protein-coupled receptor 84), represent functional processes in macrophages [121–124]. Furthermore, human macrophages express *TKT* (transketolase; *LOC108265455* in channel catfish), *CUX1* (cut like homeobox 1; *si*:*dkey-27h10.2* in channel catfish), *MMP9*, *MS4A4A*, *FBP1* (Fructose-bisphosphatase 1) and *GPR84* [59]. Only two of the top 10 genes, *LOC108265455* (transketolase) and *gpr84* have known functions in T cells [125,126]. Thus, the T5 subcluster has an indeterminate cell type with macrophage-like expression patterns (Figs 5B and S8).

Subcluster analysis was performed on the 234 myeloid cells, and five unique groups of cells with distinct expression patterns in the heat map (Figs 6A and S10) and differentially expressed genes (S7 Table) were identified. After scrutiny of differentially expressed genes, two DC clusters and three macrophage subclusters were identified. M0 subcluster (81 cells) significantly expressed the catfish gene *si*:*dkey-5n18.1*, an ortholog of human *C1QL3* (complement C1q like 3), which comes from the same gene family as *C1Q* (complement C1q). *C1Q* expression in macrophages has been implicated in the functional process of eliminating apoptotic cells [127]. The cells in the M1 subcluster (52 cells) were putatively identified as DCs as they had increased expression of *flt3* (fms related receptor tyrosine kinase 3) and *irf4a* (interferon regulatory factor 4), which have DC functions [128,129]. Subcluster M2 (40 cells) had increased expression of *lrp1ab* (low density lipoprotein receptor-related protein 1Ab) which has a function in macrophages [130]. M2 also has increased expression of *rgl1* (ral guanine nucleotide dissociation stimulator-like 1) and *LOC108277878* (sialoadhesin). The human orthologs of these genes are expressed in macrophages [59]. The subcluster M3 (39 cells) had greater expression of *cd74b and cytip* (cytohesin 1 interacting protein) which have functions in DCs [131] and is also highly expressed in human monocytes [59]. The M3 cells also expressed genes typically transcribed by DCs, *cxcr3.1* (C-X-C motif chemokine receptor 3), *batf3* (basic leucine zipper ATF-like transcription factor 3), and *znf366* (zinc finger protein 366) (Fig 6B). The subcluster M4 (22 cells) had increased expression of macrophage genes *marco*, *mafba* (MAF bZIP transcription factor B), *csf1r* (colony stimulating factor 1 receptor), *csf1* (colony stimulating factor 1), *c1qb* (complement C1q B chain) and *c1qc* (complement C1q subcomponent subunit C) [71,72,132–136].

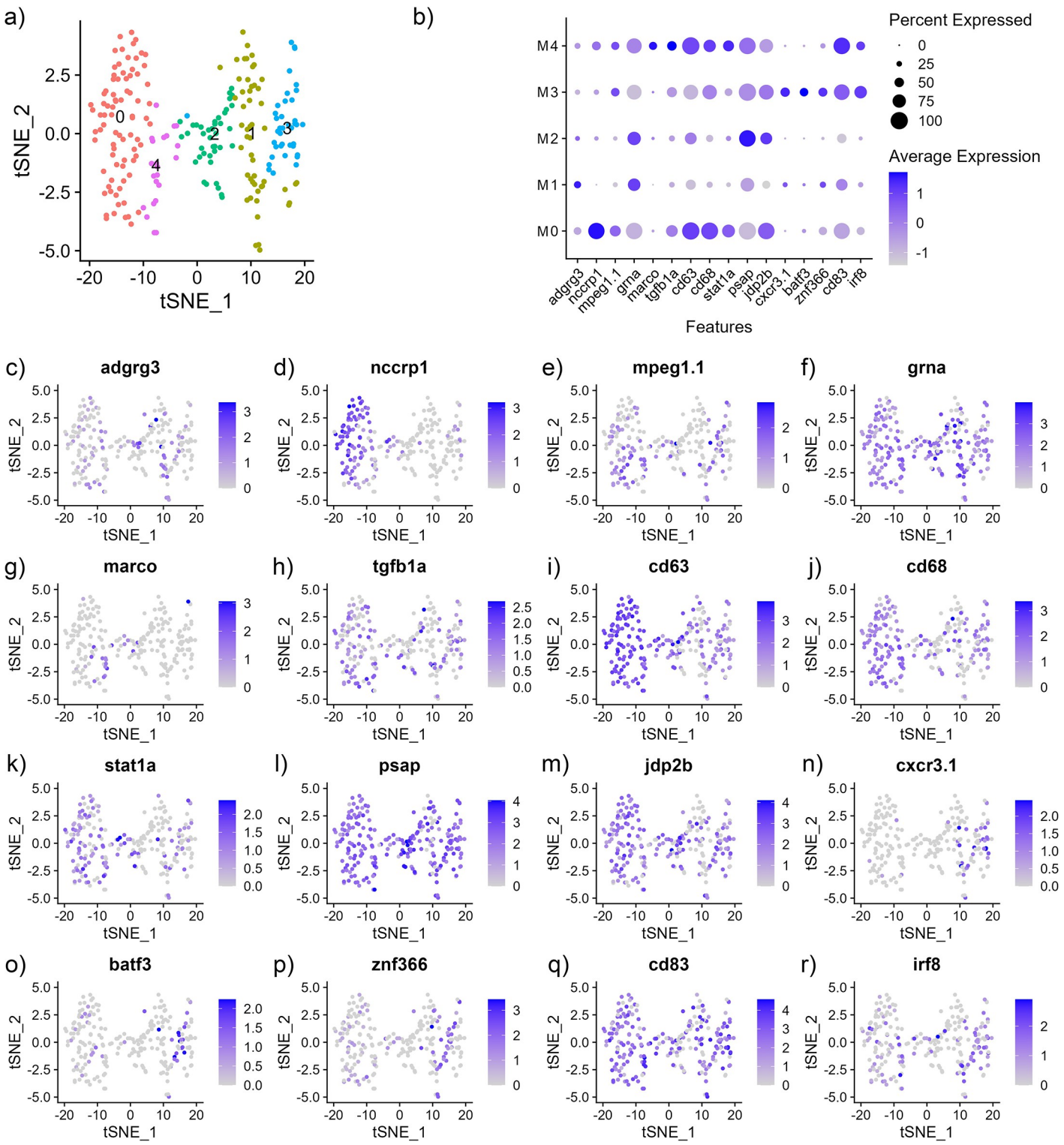

Fig 6. Subcluster analysis of myeloid cells from integrated nuclei transcriptome of spleen from channel catfish. (a) tSNE plot (b) Average expression (z-score) of cell type markers (x-axis) for each cluster (y-axis). The size of the dot represents the percentage of cells per cluster contributing to expression.

https://doi.org/10.1371/journal.pone.0309397.g006

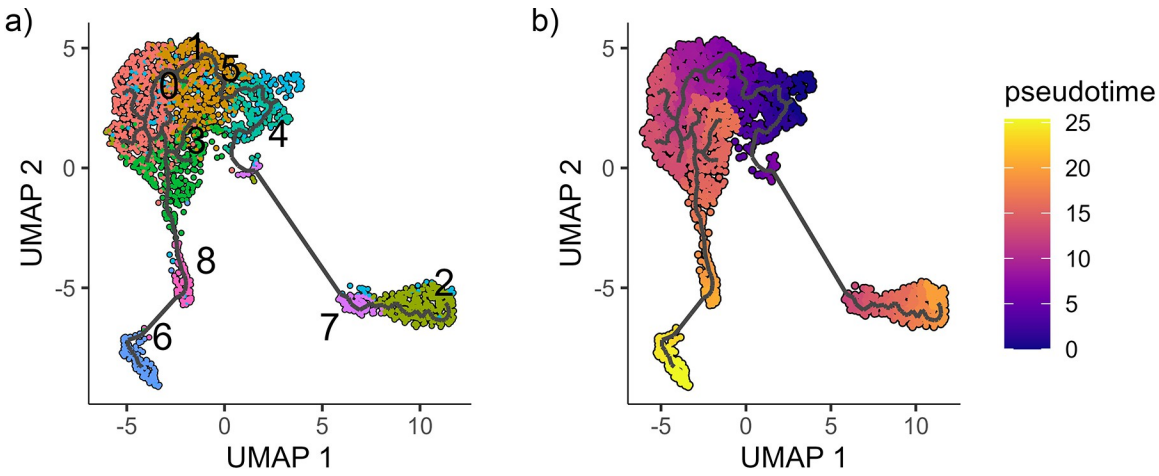

Fig 7. Trajectory analysis of B cells from integrated nuclei transcriptome of spleen from channel catfish (n = 3). (a) Predicted B cell trajectory branching and (b) predicted pseudotime determined by Monocle 3.

https://doi.org/10.1371/journal.pone.0309397.g007

Cell trajectory and pseudotime analysis

The subcluster analysis of B cells suggested that there were different stages of B cell lineage in the spleen, including immature B cells to plasma cells. The analysis with Monocle 3 was used to determine a trajectory path between clusters by using the Louvain community detection algorithm to group mutually similar cells, and then merging adjacent groups into 'super-groups'. Using this information, Monocle 3 then predicts a path that cells can take and identify branches within supergroups. The trajectory path between the B cells was projected onto the UMAP produced using Seurat (Fig 7A). Pseudotime was then calculated using nodes within subcluster B4 as root cells (Fig 7B). Cells in B4 had the higher expressions of *ebf1b*, *ikzf1* and *pax5* which suggested that they are immature B cells, and the earliest developmental time-point. The trajectory and pseudotime predict that the immature B cells can branch towards two populations (Fig 7A). One path shows a trajectory toward the mature B cells and then plasmablasts (B8) and plasma cells (B6). While, another branch connects the root cluster, B4, to subclusters B7 and B2. The B cells from B7 and B2 appear to have greater differences to the other subclusters, although, their identity is not known. These subclusters may represent circulating B cells that are not resident in the spleen.

Conclusion

Single-cell and single-nuclei RNA sequencing has enabled the characterization of a broad range of cells from a heterogenous tissue. We applied this technology to garner an understanding of the channel catfish spleen and develop an atlas that can be used for additional investigation. The spleen is considered a major lymphoid organ that filters pathogens and antigens from the blood and maintains an environment for the immune system to operate. Therefore, this atlas further provides an insight into the gene expression of erythrocytes and immune cells in this evolutionary and commercially relevant teleost species.

Supporting information

S1 Fig. Sample contribution to integrated cluster analysis. (a) tSNE map (b) Bar plot demonstrating individual sample contribution (SP1, SP2, and SP3) to the integrated dataset.
(TIF)

S2 Fig. Heat map of top differentially expressed genes for clusters generated from the integrated dataset. 0 = Erythroid, 1 = Erythroid, 2 = Erythroid, 3 = Erythroid, 4 = HSC, 5 = B Cells, 6 = Erythroid, 7 = Erythroid, 8 = T/NK Cells, 9 = B Cells, 10 = HSC, 11 = Myeloid, 12 = B Cells, 13 = B Cells, 14 = Myeloid, 15 = Endothelial Cells, 16 = Myeloid.
(TIF)

S3 Fig. Subcluster analysis of immune cells only (no erythroid cells) using the integrated dataset. (a) tSNE plot (b) Average expression (z-score) of cell type markers (x-axis) for each cluster (y-axis). The size of the dot represents the percentage of cells per cluster contributing to expression. The dotplot of cell markers identified these clusters as B cells, hematopoeitic stem cells (HSC), T and natural killer cells (T/NK cells), myeloid cells and endothelial cells.
(TIF)

S4 Fig. Heat map of top differentially expressed genes from clusters of immune cells using the integrated dataset. 0 = B Cells, 1 = HSC, 2 = HSC, 3 = B Cells, 4 = HSC, 5 = T/NK Cells, 6 = B Cells, 7 = B Cells, 8 = Myeloid, 9 = B Cells, 10 = B Cells, 11 = T/NK Cells, 12 = Myeloid, 13 = Myeloid, 14 = Endothelial Cells, 15 = HSC.
(TIF)

S5 Fig. Heat map of top differentially expressed genes from hematopoetic stem cell clusters using the integrated dataset.
(TIF)

S6 Fig. Heat map of top differentially expressed genes from B cell clusters using the integrated dataset.
(TIF)

S7 Fig. Feature maps of B cell gene expression on tSNE plots (a-x).
(TIF)

S8 Fig. Heat map of top differentially expressed genes from T/NK cell clusters using the integrated dataset.
(TIF)

S9 Fig. Feature maps of T/NK cell gene expression on tSNE plots (a-x).
(TIF)

S10 Fig. Heat map of top differentially expressed genes from myeloid cell clusters using the integrated dataset.
(TIF)

S1 Table. Top 10 differentially expressed genes for cluster generated from individual scRNAseq of spleen channel catfish samples SP1, SP2 and SP3.
(XLSX)

S2 Table. Top 10 differentially expressed genes for 17 clusters generated from scRNAseq of spleen from channel catfish samples (n = 3).
(XLSX)

S3 Table. Top 10 differentially expressed genes for sub-clusters of immune cells generated from the integrated scRNAseq of spleen from channel catfish samples (n = 3).
(XLSX)

S4 Table. Top 10 differentially expressed genes for sub-clusters of HSC cells generated from the integrated scRNAseq of spleen from channel catfish samples (n = 3).
(XLSX)

S5 Table. Top 10 differentially expressed genes for sub-clusters of B cells generated from the integrated scRNAseq of spleen from channel catfish samples (n = 3).
(XLSX)

S6 Table. Top 10 differentially expressed genes for sub-clusters of T and NK cells generated from the integrated scRNAseq of spleen from channel catfish samples (n = 3).
(XLSX)

S7 Table. Top 10 differentially expressed genes for sub-clusters of cells in the myeloid lineage generated from the integrated scRNAseq of spleen from channel catfish samples (n = 3).
(XLSX)

Acknowledgments

Mention of trade names or commercial products in this publication is solely for the purpose of providing specific information and does not imply recommendation or endorsement by the United States Department of Agriculture. The USDA is an equal opportunity provider and employer.

Author Contributions

Conceptualization: Johanna E. Aldersey, Miles D. Lange, Jason W. Abernathy.

Data curation: Johanna E. Aldersey, Jason W. Abernathy.

Formal analysis: Johanna E. Aldersey, Jason W. Abernathy.

Funding acquisition: Benjamin H. Beck, Jason W. Abernathy.

Investigation: Johanna E. Aldersey, Miles D. Lange, Jason W. Abernathy.

Methodology: Johanna E. Aldersey, Miles D. Lange, Jason W. Abernathy.

Project administration: Miles D. Lange, Benjamin H. Beck, Jason W. Abernathy.

Resources: Benjamin H. Beck, Jason W. Abernathy.

Software: Johanna E. Aldersey, Jason W. Abernathy.

Supervision: Miles D. Lange, Benjamin H. Beck, Jason W. Abernathy.

Validation: Johanna E. Aldersey, Benjamin H. Beck, Jason W. Abernathy.

Writing – original draft: Johanna E. Aldersey, Miles D. Lange, Jason W. Abernathy.

Writing – review & editing: Johanna E. Aldersey, Miles D. Lange, Benjamin H. Beck, Jason W. Abernathy.

References

1. Whyte SK. The innate immune response of finfish–A review of current knowledge. Fish & Shellfish Immunology. 2007; 23(6):1127–51. https://doi.org/10.1016/j.fsi.2007.06.005 PMID: 17980622
2. Smith NC, Rise ML, Christian SL. A comparison of the innate and adaptive immune systems in cartilaginous fish, ray-finned fish, and lobe-finned fish. Frontiers in Immunology. 2019; 10:1–23. https://doi.org/10.3389/fimmu.2019.02292 PMID: 31649660

3. Bjørgen H, Koppang EO. Anatomy of teleost fish immune structures and organs. Immunogenetics. 2021; 73(1):53–63. https://doi.org/10.1007/s00251-020-01196-0 PMID: 33426583

4. Zapata AG. The fish spleen. Fish & Shellfish Immunology. 2024; 144:1–10. https://doi.org/10.1016/j.fsi.2023.109280 PMID: 38086514

5. Dickerson HW, Findly RC. Vertebrate adaptive immunity-comparative unsights from a teleost model. Frontiers in Immunology. 2017. https://doi.org/10.3389/fimmu.2017.01379 PMID: 29123524

6. Hu CB, Wang J, Hong Y, Li H, Fan DD, Lin AF, et al. Single-cell transcriptome profiling reveals diverse immune cell populations and their responses to viral infection in the spleen of zebrafish. Faseb j. 2023; 37(6). https://doi.org/10.1096/fj.202201505RRRR PMID: 37227178

7. Danilova N, Bussmann J, Jekosch K, Steiner LA. The immunoglobulin heavy-chain locus in zebrafish: identification and expression of a previously unknown isotype, immunoglobulin Z. Nature Immunology. 2005; 6(3):295–302. https://doi.org/10.1038/ni1166 PMID: 15685175

8. Xu J, Zhang X, Luo Y, Wan X, Yao Y, Zhang L, et al. IgM and IgD heavy chains of yellow catfish (*Pelteobagrus fulvidraco*): Molecular cloning, characterization and expression analysis in response to bacterial infection. Fish & Shellfish Immunology. 2019; 84:233–43. https://doi.org/10.1016/j.fsi.2018.10.012 PMID: 30300742

9. Zhang Y-A, Salinas I, Li J, Parra D, Bjork S, Xu Z, et al. IgT, a primitive immunoglobulin class specialized in mucosal immunity. Nature Immunology. 2010; 11(9):827–35. https://doi.org/10.1038/ni.1913 PMID: 20676094

10. Bengtén E, Quiniou SM-A, Stuge TB, Katagiri T, Miller NW, Clem LW, et al. The IgH locus of the channel catfish, *Ictalurus punctatus*, contains multiple constant region gene sequences: Different genes encode heavy chains of membrane and secreted IgD. The Journal of Immunology. 2002; 169 (5):2488–97. https://doi.org/10.4049/jimmunol.169.5.2488 PMID: 12193718

11. Quick stats: livestock and animals [Internet]. 2023 [cited 23/04/2024]. Available from: https://www.nass.usda.gov/Statistics_by_Subject/index.php?sector=ANIMALS%20&%20PRODUCTS.

12. Abdelrahman HA, Hemstreet WG, Roy LA, Hanson TR, Beck BH, Kelly AM. Epidemiology and economic impact of disease-related losses on commercial catfish farms: A seven-year case study from Alabama, USA. Aquaculture. 2023. https://doi.org/10.1016/j.aquaculture.2022.739206

13. Peatman E, Li C, Peterson BC, Straus DL, Farmer BD, Beck BH. Basal polarization of the mucosal compartment in Flavobacterium columnare susceptible and resistant channel catfish (*Ictalurus punctatus)*. Molecular Immunology. 2013; 56(4):317–27. https://doi.org/10.1016/j.molimm.2013.04.014 PMID: 23895942

14. Lange MD, Abernathy J, Farmer BD. Evaluation of a recombinant *Flavobacterium columnare* DnaK protein vaccine as a means of protection against columnaris disease in channel catfish (*Ictalurus punctatus*). Frontiers in Immunology. 2019; 10. https://doi.org/10.3389/fimmu.2019.01175 PMID: 31244827

15. Li C, Zhang Y, Wang R, Lu J, Nandi S, Mohanty S, et al. RNA-seq analysis of mucosal immune responses reveals signatures of intestinal barrier disruption and pathogen entry following Edwardsiella ictaluri infection in channel catfish, Ictalurus punctatus. Fish & Shellfish Immunology. 2012; 32(5):816–27. https://doi.org/10.1016/j.fsi.2012.02.004 PMID: 22366064

16. Li X, Wang C-Y. From bulk, single-cell to spatial RNA sequencing. International Journal of Oral Science. 2021; 13(1):36. https://doi.org/10.1038/s41368-021-00146-0 PMID: 34782601

17. Sun J, Ruiz Daniels R, Balic A, Andresen AMS, Bjørgen H, Dobie R, et al. Cell atlas of the Atlantic salmon spleen reveals immune cell heterogeneity and cell-specific responses to bacterial infection. Fish & Shellfish Immunology. 2024; 145. https://doi.org/10.1016/j.fsi.2024.109358 PMID: 38176627

18. Lange MD, Churchman EM, Wise AL, Bruce TJ. A recombinant 9E1 monoclonal antibody binds membrane and soluble channel catfish immunoglobulin M. Fish and Shellfish Immunology Reports. 2023; 4. https://doi.org/10.1016/j.fsirep.2023.100086 PMID: 36895760

19. Rychlik W, Spencer WJ, Rhoads RE. Optimization of the annealing temperature for DNA amplification in vitro. Nucleic Acids Research. 1990; 18(21):6409–12. https://doi.org/10.1093/nar/18.21.6409 PMID: 2243783

20. Wilson MR, Marcuz A, van Ginkel F, Miller NW, Clem LW, Middleton D, et al. The immunoglobulin M heavy chain constant region gene of the channel catfish, Ictalurus punctatus: an unusual mRNA splice pattern produces the membrane form of the molecule. Nucleic Acids Research. 1990; 18(17):5227–33. https://doi.org/10.1093/nar/18.17.5227 PMID: 2119496

21. Hao Y, Stuart T, Kowalski MH, Choudhary S, Hoffman P, Hartman A, et al. Dictionary learning for integrative, multimodal and scalable single-cell analysis. Nature Biotechnology. 2024; 42(2):293–304. https://doi.org/10.1038/s41587-023-01767-y PMID: 37231261

22. Cao J, Spielmann M, Qiu X, Huang X, Ibrahim DM, Hill AJ, et al. The single-cell transcriptional landscape of mammalian organogenesis. Nature. 2019; 566(7745):496–502. https://doi.org/10.1038/s41586-019-0969-x PMID: 30787437

23. Genetet S, Desrames A, Chouali Y, Ripoche P, Lopez C, Mouro-Chanteloup I. Stomatin modulates the activity of the Anion Exchanger 1 (AE1, SLC4A1). Scientific Reports. 2017; 7(1):46170. https://doi.org/10.1038/srep46170 PMID: 28387307

24. Zheng W-W, Dong X-M, Yin R-H, Xu F-F, Ning H-M, Zhang M-J, et al. EDAG Positively Regulates Erythroid Differentiation and Modifies GATA1 Acetylation Through Recruiting p300. Stem Cells. 2014; 32 (8):2278–89. https://doi.org/10.1002/stem.1723 PMID: 24740910

25. Cobaleda C, Schebesta A, Delogu A, Busslinger M. Pax5: the guardian of B cell identity and function. Nature Immunology. 2007; 8(5):463–70. https://doi.org/10.1038/ni1454 PMID: 17440452

26. Taylor EB, Wilson M, Bengten E. The Src tyrosine kinase Lck binds to CD2, CD4-1, and CD4-2 T cell co-receptors in channel catfish, Ictalurus punctatus. Molecular Immunology. 2015; 66(2):126–38. Epub 20150312. https://doi.org/10.1016/j.molimm.2015.02.023 PMID: 25771179.

27. Uhl LFK, Cai H, Oram SL, Mahale JN, MacLean AJ, Mazet JM, et al. Interferon-γ couples CD8+ T cell avidity and differentiation during infection. Nature Communications. 2023; 14(1):6727. https://doi.org/10.1038/s41467-023-42455-4 PMID: 37872155

28. Cui L, Moraga I, Lerbs T, Van Neste C, Wilmes S, Tsutsumi N, et al. Tuning MPL signaling to influence hematopoietic stem cell differentiation and inhibit essential thrombocythemia progenitors. Proceedings of the National Academy of Sciences. 2021; 118(2):e2017849118. https://doi.org/10.1073/pnas.2017849118 PMID: 33384332

29. Unnisa Z, Clark JP, Roychoudhury J, Thomas E, Tessarollo L, Copeland NG, et al. Meis1 preserves hematopoietic stem cells in mice by limiting oxidative stress. Blood. 2012; 120(25):4973–81. https://doi.org/10.1182/blood-2012-06-435800 PMID: 23091297

30. de Pater E, Kaimakis P, Vink CS, Yokomizo T, Yamada-Inagawa T, van der Linden R, et al. Gata2 is required for HSC generation and survival. Journal of Experimental Medicine. 2013; 210(13):2843–50. https://doi.org/10.1084/jem.20130751 PMID: 24297996

31. Hsiao C-C, Chu T-Y, Wu C-J, van den Biggelaar M, Pabst C, Hébert J, et al. The adhesion G protein-coupled receptor GPR97/ADGRG3 is expressed in human granulocytes and triggers antimicrobial effector functions. Frontiers in Immunology. 2018; 9. https://doi.org/10.3389/fimmu.2018.02830 PMID: 30559745

32. Palencia-Desai S, Kohli V, Kang J, Chi NC, Black BL, Sumanas S. Vascular endothelial and endocardial progenitors differentiate as cardiomyocytes in the absence of Etsrp/Etv2 function. Development. 2011; 138(21):4721–32. https://doi.org/10.1242/dev.064998 PMID: 21989916

33. Chen C-W, Huang N-K, Lee Y-L, Fan C-K, Chen Y-C, Liu C-W, Huang H-M. Activin A downregulates the CD69-MT2A axis via p38MAPK to induce erythroid differentiation that sensitizes BCR-ABL-positive cells to imatinib. Experimental Cell Research. 2022; 417(2). https://doi.org/10.1016/j.yexcr.2022.113219 PMID: 35643179

34. Duff MR Jr, Redzic JS, Ryan LP, Paukovich N, Zhao R, Nix JC, et al. Structure, dynamics and function of the evolutionarily changing biliverdin reductase B family. The Journal of Biochemistry. 2020; 168 (2):191–202. https://doi.org/10.1093/jb/mvaa039 PMID: 32246827

35. Phillips JD. Heme biosynthesis and the porphyrias. Molecular Genetics and Metabolism. 2019; 128 (3):164–77. https://doi.org/10.1016/j.ymgme.2019.04.008 PMID: 31326287

36. D'Alessandro A, Hay A, Dzieciatkowska M, Brown BC, Morrison EJ, Hansen KC, Zimring JC. Protein-L-isoaspartate O-methyltransferase is required for in vivo control of oxidative damage in red blood cells. Haematologica. 2021; 106(10):2726–39. https://doi.org/10.3324/haematol.2020.266676 PMID: 33054131

37. Vallese F, Kim K, Yen LY, Johnston JD, Noble AJ, Calì T, Clarke OB. Architecture of the human erythrocyte ankyrin-1 complex. Nature Structural and Molecular Biology. 2022; 29(7):706–18. https://doi.org/10.1038/s41594-022-00792-w PMID: 35835865

38. Cantù C, Ierardi R, Alborelli I, Fugazza C, Cassinelli L, Piconese S, et al. Sox6 enhances erythroid differentiation in human erythroid progenitors. Blood. 2011; 117(13):3669–79. https://doi.org/10.1182/blood-2010-04-282350 PMID: 21263153

39. Bouthelier A, Fernández-Arroyo L, Mesa-Ciller C, Cibrian D, Martín-Cófreces NB, Castillo-González R, et al. Erythroid SLC7A5/SLC3A2 amino acid carrier controls red blood cell size and maturation. iScience. 2023; 26(1). https://doi.org/10.1016/j.isci.2022.105739 PMID: 36582828

40. Cooney JD, Hildick-Smith GJ, Shafizadeh E, McBride PF, Carroll KJ, Anderson H, et al. Teleost growth factor independence (gfi) genes differentially regulate successive waves of hematopoiesis. Developmental Biology. 2013; 373(2):431–41. https://doi.org/10.1016/j.ydbio.2012.08.015 PMID: 22960038

41. Kissa K, Murayama E, Zapata A, Cortés A, Perret E, Machu C, Herbomel P. Live imaging of emerging hematopoietic stem cells and early thymus colonization. Blood. 2008; 111(3):1147–56. https://doi.org/10.1182/blood-2007-07-099499 PMID: 17934068

42. Gekas C, Graf T. CD41 expression marks myeloid-biased adult hematopoietic stem cells and increases with age. Blood. 2013; 121(22):4463–72. https://doi.org/10.1182/blood-2012-09-457929 PMID: 23564910

43. Dumon S, Walton DS, Volpe G, Wilson N, Dassé E, Pozzo WD, et al. Itga2b regulation at the onset of definitive hematopoiesis and commitment to differentiation. PLOS ONE. 2012; 7(8). https://doi.org/10.1371/journal.pone.0043300 PMID: 22952660

44. Wang J, Liu Z, Zhang S, Wang X, Bai H, Xie M, et al. Lineage marker expression on mouse hematopoietic stem cells. Experimental Hematology. 2019; 76. https://doi.org/10.1016/j.exphem.2019.07.001 PMID: 31299288

45. Kobayashi I, Kondo M, Yamamori S, Kobayashi-Sun J, Taniguchi M, Kanemaru K, et al. Enrichment of hematopoietic stem/progenitor cells in the zebrafish kidney. Scientific Reports. 2019; 9. https://doi.org/10.1038/s41598-019-50672-5 PMID: 31578390

46. Kocabas F, Zheng J, Thet S, Copeland NG, Jenkins NA, DeBerardinis RJ, et al. Meis1 regulates the metabolic phenotype and oxidant defense of hematopoietic stem cells. Blood. 2012; 120(25):4963–72. https://doi.org/10.1182/blood-2012-05-432260 PMID: 22995899

47. Edholm E-S, Wilson M, Sahoo M, Miller NW, Pilström L, Wermenstam NE, Bengtén E. Identification of Igσ and Igλ in channel catfish, *Ictalurus punctatus*, and Igλ in Atlantic cod, *Gadus morhua*. Immunogenetics. 2009; 61(5):353–70. https://doi.org/10.1007/s00251-009-0365-z PMID: 19333591

48. Edholm E-S, Wilson M, Bengten E. Immunoglobulin light (IgL) chains in ectothermic vertebrates. Developmental & Comparative Immunology. 2011; 35(9):906–15. https://doi.org/10.1016/j.dci.2011.01.012 PMID: 21256861

49. Zwollo P. Dissecting teleost B cell differentiation using transcription factors. Developmental & Comparative Immunology. 2011; 35(9):898–905. https://doi.org/10.1016/j.dci.2011.01.009 PMID: 21251922

50. Solem ST, Stenvik J. Antibody repertoire development in teleosts—a review with emphasis on salmonids and *Gadus morhua* L. Developmental & Comparative Immunology. 2006; 30(1):57–76. https://doi.org/10.1016/j.dci.2005.06.007 PMID: 16084588

51. Brooks JF, Tan C, Mueller JL, Hibiya K, Hiwa R, Vykunta V, Zikherman J. Negative feedback by NUR77/Nr4a1 restrains B cell clonal dominance during early T-dependent immune responses. Cell Reports. 2021; 36(9). https://doi.org/10.1016/j.celrep.2021.109645 PMID: 34469720

52. Westbrook L, Johnson AC, Regner KR, Williams JM, Mattson DL, Kyle PB, et al. Genetic susceptibility and loss of Nr4a1 enhances macrophage-mediated renal injury in CKD. Journal of the American Society of Nephrology. 2014; 25(11). https://doi.org/10.1681/ASN.2013070786 PMID: 24722447

53. Shibasaki Y, Afanasyev S, Fernández-Montero A, Ding Y, Watanabe S, Takizawa F, et al. Cold-blooded vertebrates evolved organized germinal center–like structures. Science Immunology. 2023; 8(90). https://doi.org/10.1126/sciimmunol.adf1627 PMID: 37910630

54. Vigliano FA, Bermúdez R, Quiroga MI, Nieto JM. Evidence for melano-macrophage centres of teleost as evolutionary precursors of germinal centres of higher vertebrates: An immunohistochemical study. Fish & Shellfish Immunology. 2006; 21(4):467–71. https://doi.org/10.1016/j.fsi.2005.12.012 PMID: 16533606

55. Shahaf G, Gross AJ, Sternberg-Simon M, Kaplan D, DeFranco AL, Mehr R. Lyn deficiency affects B-cell maturation as well as survival. European Journal of Immunology. 2012; 42(2):511–21. https://doi.org/10.1002/eji.201141940 PMID: 22057631

56. Dornburg A, Yoder JA. On the relationship between extant innate immune receptors and the evolutionary origins of jawed vertebrate adaptive immunity. Immunogenetics. 2022; 74(1):111–28. https://doi.org/10.1007/s00251-021-01232-7 PMID: 34981186

57. Kobayashi S, Phung HT, Tayama S, Kagawa Y, Miyazaki H, Yamamoto Y, et al. Fatty acid-binding protein 3 regulates differentiation of IgM-producing plasma cells. The FEBS Journal. 2021; 288(4):1130–41. https://doi.org/10.1111/febs.15460 PMID: 32578350

58. Duan M, Nguyen DC, Joyner CJ, Saney CL, Tipton CM, Andrews J, et al. Understanding heterogeneity of human bone marrow plasma cell maturation and survival pathways by single-cell analyses. Cell Reports. 2023; 42(7). https://doi.org/10.1016/j.celrep.2023.112682 PMID: 37355988

59. Uhlen M, Karlsson MJ, Zhong W, Tebani A, Pou C, Mikes J, et al. A genome-wide transcriptomic analysis of protein-coding genes in human blood cells. Science. 2019; 366(6472). https://doi.org/10.1126/science.aax9198 PMID: 31857451

60. Liu B, Li Z. Endoplasmic reticulum HSP90b1 (gp96, grp94) optimizes B-cell function via chaperoning integrin and TLR but not immunoglobulin. Blood. 2008; 112(4):1223–30. https://doi.org/10.1182/blood-2008-03-143107 PMID: 18509083

61. Alexander DR. The CD45 tyrosine phosphatase: a positive and negative regulator of immune cell function. Seminars in Immunology. 2000; 12(4):349–59. https://doi.org/10.1006/smim.2000.0218 PMID: 10995582

62. Giezeman-Smits KM, Gorter A, van Vlierberghe RLP, v. Eendenburg JDH, Eggermont AMM, Fleuren GJ, Kuppen PJK. The regulatory role of CD45 on rat NK cells in target cell lysis. The Journal of Immunology. 1999; 163(1):71–6. https://doi.org/10.4049/jimmunol.163.1.71 PMID: 10384101

63. Kountikov E, Nayak D, Wilson M, Miller NW, Bengtén E. Expression of alternatively spliced CD45 isoforms by channel catfish clonal T and B cells is dependent on activation state of the cell and regulated by protein synthesis and degradation. Developmental & Comparative Immunology. 2010; 34 (10):1109–18. https://doi.org/10.1016/j.dci.2010.06.003 PMID: 20547174

64. Woolf E, Brenner O, Goldenberg D, Levanon D, Groner Y. Runx3 regulates dendritic epidermal T cell development. Developmental Biology. 2007; 303(2):703–14. https://doi.org/10.1016/j.ydbio.2006.12.005 PMID: 17222403

65. Thompson SB, Sandor AM, Lui V, Chung JW, Waldman MM, Long RA, et al. Formin-like 1 mediates effector T cell trafficking to inflammatory sites to enable T cell-mediated autoimmunity. eLife. 2020; 9. https://doi.org/10.7554/eLife.58046 PMID: 32510333

66. Masuda K, Ripley B, Nyati KK, Dubey PK, Zaman MM-U, Hanieh H, et al. Arid5a regulates naive CD4 + T cell fate through selective stabilization of Stat3 mRNA. Journal of Experimental Medicine. 2016; 213(4):605–19. https://doi.org/10.1084/jem.20151289 PMID: 27022145

67. Elizondo DM, Andargie TE, Haddock NL, Boddie TA, Lipscomb MW. Drebrin 1 in dendritic cells regulates phagocytosis and cell surface receptor expression through recycling for efficient antigen presentation. Immunology. 2019; 156(2):136–46. https://doi.org/10.1111/imm.13010 PMID: 30317558

68. Law M, Lee Y, Morales JL, Ning G, Huang W, Pabon J, et al. Cutting Edge: Drebrin-Regulated Actin Dynamics Regulate IgE-Dependent Mast Cell Activation and Allergic Responses. The Journal of Immunology. 2015; 195(2):426–30. https://doi.org/10.4049/jimmunol.1401442 PMID: 26056254

69. Ismailova A, Salehi-Tabar R, Dimitrov V, Memari B, Barbier C, White JH. Identification of a forkhead box protein transcriptional network induced in human neutrophils in response to inflammatory stimuli. Frontiers in Immunology. 2023; 14. https://doi.org/10.3389/fimmu.2023.1123344 PMID: 36756115

70. Jiang W, Ma C, Bai J, Du X. Macrophage SAMSN1 protects against sepsis-induced acute lung injury in mice. Redox Biology. 2022; 56. https://doi.org/10.1016/j.redox.2022.102432 PMID: 35981417

71. Bakri Y, Sarrazin S, Mayer UP, Tillmanns S, Nerlov C, Boned A, Sieweke MH. Balance of MafB and PU.1 specifies alternative macrophage or dendritic cell fate. Blood. 2005; 105(7):2707–16. https://doi.org/10.1182/blood-2004-04-1448 PMID: 15598817

72. Chen Q, Lu X-J, Chen J. Identification and functional characterization of the CSF1R gene from grass carp *Ctenopharyngodon idellus* and its use as a marker of monocytes/macrophages. Fish & Shellfish Immunology. 2015; 45(2):386–98. https://doi.org/10.1016/j.fsi.2015.04.029 PMID: 25956721

73. Mun SH, Park PSU, Park-Min K-H. The M-CSF receptor in osteoclasts and beyond. Experimental & Molecular Medicine. 2020; 52(8):1239–54. https://doi.org/10.1038/s12276-020-0484-z PMID: 32801364

74. Bartel Y, Bauer B, Steinle A. Modulation of NK cell function by genetically coupled c-type lectin-like receptor/ligand pairs encoded in the human natural killer gene complex. Frontiers in Immunology. 2013. https://doi.org/10.3389/fimmu.2013.00362 PMID: 24223577

75. Peterson EE, Barry KC. The natural killer-dendritic cell immune axis in anti-cancer immunity and immunotherapy. Frontiers in Immunology. 2020; 11. https://doi.org/10.3389/fimmu.2020.621254 PMID: 33613552

76. Watowich SS, Liu Y-J. Mechanisms regulating dendritic cell specification and development. Immunological Reviews. 2010; 238(1):76–92. https://doi.org/10.1111/j.1600-065X.2010.00949.x PMID: 20969586

77. Nicholls SE, Winter S, Mottram R, Miyan JA, Whetton AD. Flt3 ligand can promote survival and macrophage development without proliferation in myeloid progenitor cells. Experimental Hematology. 1999; 27(4):663–72. https://doi.org/10.1016/s0301-472x(98)00072-1 PMID: 10210324

78. Cheng W-L, Zhang Q, Li B, Cao J-L, Jiao L, Chao S-P, et al. PAK1 silencing attenuated proinflammatory macrophage activation and foam cell formation by increasing PPAR γ expression. Oxidative Medicine and Cellular Longevity. 2021; 2021. https://doi.org/10.1155/2021/6957900 PMID: 34603600

79. Uzureau S, Coquerelle C, Vermeiren C, Uzureau P, Van Acker A, Pilotte L, et al. Apolipoproteins L control cell death triggered by TLR3/TRIF signaling in dendritic cells. European Journal of Immunology. 2016; 46(8):1854–66. https://doi.org/10.1002/eji.201546252 PMID: 27198486

80. Zhang R, Kang R, Tang D. The STING1 network regulates autophagy and cell death. Signal Transduction and Targeted Therapy. 2021; 6(1):208. https://doi.org/10.1038/s41392-021-00613-4 PMID: 34078874

81. Heinz LX, Lee J, Kapoor U, Kartnig F, Sedlyarov V, Papakostas K, et al. TASL is the SLC15A4-associated adaptor for IRF5 activation by TLR7–9. Nature. 2020; 581(7808):316–22. https://doi.org/10.1038/s41586-020-2282-0 PMID: 32433612

82. Han SM, Na HY, Ham O, Choi W, Sohn M, Ryu SH, et al. TCF4-Targeting miR-124 is differentially expressed amongst dendritic cell subsets. Immune Network. 2016; 16(1):61–74. https://doi.org/10.4110/in.2016.16.1.61 PMID: 26937233

83. Strong SJ, Mueller MG, Litman RT, Hawke NA, Haire RN, Miracle AL, et al. A novel multigene family encodes diversified variable regions. Proceedings of the National Academy of Sciences. 1999; 96 (26):15080–5. https://doi.org/10.1073/pnas.96.26.15080 PMID: 10611341.

84. Yoder JA, Mueller MG, Wei S, Corliss BC, Prather DM, Willis T, et al. Immune-type receptor genes in zebrafish share genetic and functional properties with genes encoded by the mammalian leukocyte receptor cluster. Proceedings of the National Academy of Sciences. 2001; 98(12):6771–6. https://doi.org/10.1073/pnas.121101598 PMID: 11381126

85. Dong X, Ye Z, Song L, Su B, Zhao H, Peatman E, Li C. Expression profile analysis of two cathepsin S in channel catfish (*Ictalurus punctatus*) mucosal tissues following bacterial challenge. Fish & Shellfish Immunology. 2016; 48:112–8. https://doi.org/10.1016/j.fsi.2015.11.030 PMID: 26626584

86. Okuda KS, Hogan BM. Endothelial cell dynamics in vascular development: Insights from live-imaging in zebrafish. Frontiers in Physiology. 2020; 11. https://doi.org/10.3389/fphys.2020.00842 PMID: 32792978

87. Larson JD, Wadman SA, Chen E, Kerley L, Clark KJ, Eide M, et al. Expression of VE-cadherin in zebrafish embryos: A new tool to evaluate vascular development. Developmental Dynamics. 2004; 231 (1):204–13. https://doi.org/10.1002/dvdy.20102 PMID: 15305301

88. Shen Y, Wang D, Zhao J, Chen X. Fish red blood cells express immune genes and responses. Aquaculture and Fisheries. 2018; 3(1):14–21. https://doi.org/10.1016/j.aaf.2018.01.001

89. Lee RD, Munro SA, Knutson TP, LaRue RS, Heltemes-Harris LM, Farrar MA. Single-cell analysis identifies dynamic gene expression networks that govern B cell development and transformation. Nature Communications. 2021; 12(1):6843. https://doi.org/10.1038/s41467-021-27232-5 PMID: 34824268

90. Morgan D, Tergaonkar V. Unraveling B cell trajectories at single cell resolution. Trends in Immunology. 2022; 43(3):210–29. https://doi.org/10.1016/j.it.2022.01.003 PMID: 35090788

91. Hu H, Wang B, Borde M, Nardone J, Maika S, Allred L, et al. Foxp1 is an essential transcriptional regulator of B cell development. Nature Immunology. 2006; 7(8):819–26. https://doi.org/10.1038/ni1358 PMID: 16819554

92. Kirstetter P, Thomas M, Dierich A, Kastner P, Chan S. Ikaros is critical for B cell differentiation and function. European Journal of Immunology. 2002; 32(3):720–30. https://doi.org/10.1002/1521-4141(200203)32:3<720::AID-IMMU720>3.0.CO;2-P PMID: 11870616

93. Garrett-Sinha LA. Review of Ets1 structure, function, and roles in immunity. Cellular and Molecular Life Sciences. 2013; 70(18):3375–90. https://doi.org/10.1007/s00018-012-1243-7 PMID: 23288305

94. Vazquez MI, Catalan-Dibene J, Zlotnik A. B cells responses and cytokine production are regulated by their immune microenvironment. Cytokine. 2015; 74(2):318–26. https://doi.org/10.1016/j.cyto.2015.02.007 PMID: 25742773

95. Granja AG, Perdiguero P, Martín-Martín A, Díaz-Rosales P, Soleto I, Tafalla C. Rainbow trout IgM+ B cells preferentially respond to thymus-independent antigens but are activated by CD40L. Frontiers in Immunology. 2019; 10. https://doi.org/10.3389/fimmu.2019.02902 PMID: 31921163

96. Grasseau A, Boudigou M, Michée-Cospolite M, Delaloy C, Mignen O, Jamin C, et al. The diversity of the plasmablast signature across species and experimental conditions: A meta-analysis. Immunology. 2021; 164(1):120–34. https://doi.org/10.1111/imm.13344 PMID: 34041745

97. Perdiguero P, Goméz-Esparza MC, Martín D, Bird S, Soleto I, Morel E, et al. Insights into the evolution of the prdm1/Blimp1 gene family in teleost fish. Frontiers in Immunology. 2020; 11. https://doi.org/10.3389/fimmu.2020.596975 PMID: 33193451

98. Todd DJ, McHeyzer-Williams LJ, Kowal C, Lee A-H, Volpe BT, Diamond B, et al. XBP1 governs late events in plasma cell differentiation and is not required for antigen-specific memory B cell development. Journal of Experimental Medicine. 2009; 206(10):2151–9. https://doi.org/10.1084/jem.20090738 PMID: 19752183

99. Burute M, Gottimukkala K, Galande S. Chromatin organizer SATB1 is an important determinant of T-cell differentiation. Immunology & Cell Biology. 2012; 90(9):852–9. https://doi.org/10.1038/icb.2012.28 PMID: 22710879

100. Williams JW, Yau D, Sethakorn N, Kach J, Reed EB, Moore TV, et al. RGS3 controls T lymphocyte migration in a model of Th2-mediated airway inflammation. American Journal of Physiology-Lung

Cellular and Molecular Physiology. 2013; 305(10). https://doi.org/10.1152/ajplung.00214.2013 PMID: 24077945.

101. Harly C, Kenney D, Wang Y, Ding Y, Zhao Y, Awasthi P, Bhandoola A. A shared regulatory element controls the initiation of Tcf7 expression during Early T cell and innate lymphoid cell developments. Frontiers in Immunology. 2020; 11. https://doi.org/10.3389/fimmu.2020.00470 PMID: 32265924

102. Horiuchi S, Wu H, Liu W-C, Schmitt N, Provot J, Liu Y, et al. Tox2 is required for the maintenance of GC T_{FH} cells and the generation of memory T_{FH} cells. Science Advances. 2021; 7(41). https://doi.org/10.1126/sciadv.abj1249 PMID: 34623911

103. Liu J, Wang Z, Hao S, Wang F, Yao Y, Zhang Y, et al. Tcf1 sustains the expression of multiple regulators in promoting early natural killer cell development. Frontiers in Immunology. 2021; 12. https://doi.org/10.3389/fimmu.2021.791220 PMID: 34917097

104. Seo H, Chen J, González-Avalos E, Samaniego-Castruita D, Das A, Wang YH, et al. TOX and TOX2 transcription factors cooperate with NR4A transcription factors to impose $CD8^+$ T cell exhaustion. Proceedings of the National Academy of Sciences. 2019; 116(25):12410–5. https://doi.org/10.1073/pnas.1905675116 PMID: 31152140

105. Vong QP, Leung W-H, Houston J, Li Y, Rooney B, Holladay M, et al. TOX2 regulates human natural killer cell development by controlling T-BET expression. Blood. 2014; 124(26):3905–13. https://doi.org/10.1182/blood-2014-06-582965 PMID: 25352127

106. Niu H, Wang H. TOX regulates T lymphocytes differentiation and its function in tumor. Frontiers in Immunology. 2023; 14. https://doi.org/10.3389/fimmu.2023.990419 PMID: 36969216

107. Han J, Wan M, Ma Z, He P. The TOX subfamily: all-round players in the immune system. Clinical and Experimental Immunology. 2022; 208(3):268–80. https://doi.org/10.1093/cei/uxac037 PMID: 35485425

108. Rakhra G, Rakhra G. Zinc finger proteins: insights into the transcriptional and post transcriptional regulation of immune response. Molecular Biology Reports. 2021; 48(7):5735–43. https://doi.org/10.1007/s11033-021-06556-x PMID: 34304391

109. Yh Chien, Bonneville M. Gamma delta T cell receptors. Cellular and Molecular Life Sciences CMLS. 2006; 63(18):2089–94. https://doi.org/10.1007/s00018-006-6020-z PMID: 17003966

110. Dexiu C, Xianying L, Yingchun H, Jiafu L. Advances in CD247. Scandinavian Journal of Immunology. 2022; 96(1). https://doi.org/10.1111/sji.13170 PMID: 35388926

111. Ashouri JF, Lo W-L, Nguyen TTT, Shen L, Weiss A. ZAP70, too little, too much can lead to autoimmunity. Immunological Reviews. 2022; 307(1):145–60. https://doi.org/10.1111/imr.13058 PMID: 34923645

112. Imbratta C, Hussein H, Andris F, Verdeil G. c-MAF, a Swiss Army Knife for Tolerance in Lymphocytes. Frontiers in Immunology. 2020. https://doi.org/10.3389/fimmu.2020.00206 PMID: 32117317

113. Liu P, Li P, Burke S. Critical roles of Bcl11b in T-cell development and maintenance of T-cell identity. Immunological Reviews. 2010; 238(1):138–49. https://doi.org/10.1111/j.1600-065X.2010.00953.x PMID: 20969590

114. Wan F, Hu CB, Ma JX, Gao K, Xiang LX, Shao JZ. Characterization of γδ T cells from zebrafish provides insights into their important role in adaptive humoral immunity. Frontiers in Immunology. 2016; 7. https://doi.org/10.3389/fimmu.2016.00675 PMID: 28119690; PubMed Central PMCID: PMC5220103.

115. Ribot JC, Lopes N, Silva-Santos B. γδ T cells in tissue physiology and surveillance. Nature Reviews Immunology. 2021; 21(4):221–32. https://doi.org/10.1038/s41577-020-00452-4 PMID: 33057185

116. Roda-Navarro P, Reyburn HT. The traffic of the NKG2D/Dap10 receptor complex during natural killer (NK) cell activation. Journal of Biological Chemistry. 2009; 284(24):16463–72. Epub https://doi.org/10.1074/jbc.M808561200 PMID: 19329438.

117. Nagy N, Cerboni C, Mattsson K, Maeda A, Gogolák P, Sümegi J, et al. SH2D1A and slam protein expression in human lymphocytes and derived cell lines. International Journal of Cancer. 2000; 88 (3):439–47. PMID: 11054674

118. Wowk ME, Trapani JA. Cytotoxic activity of the lymphocyte toxin granzyme B. Microbes and Infection. 2004; 6(8):752–8. https://doi.org/10.1016/j.micinf.2004.03.008 PMID: 15207822

119. Duquette D, Harmon C, Zaborowski A, Michelet X, O'Farrelly C, Winter D, et al. Human granzyme K is a feature of innate T cells in blood, tissues, and tumors, responding to cytokines rather than TCR stimulation. The Journal of Immunology. 2023; 211(4):633–47. https://doi.org/10.4049/jimmunol.2300083 PMID: 37449888

120. Yamaguchi T, Takizawa F, Furihata M, Soto-Lampe V, Dijkstra JM, Fischer U. Teleost cytotoxic T cells. Fish & Shellfish Immunology. 2019; 95:422–39. https://doi.org/10.1016/j.fsi.2019.10.041 PMID: 31669897

121. Cabrera S, Maciel M, Hernández-Barrientos D, Calyeca J, Gaxiola M, Selman M, Pardo A. Delayed resolution of bleomycin-induced pulmonary fibrosis in absence of MMP13 (collagenase 3). American Journal of Physiology-Lung Cellular and Molecular Physiology. 2019; 316(5):961–76. https://doi.org/10.1152/ajplung.00455.2017 PMID: 30785343

122. Tekin C, Aberson HL, Waasdorp C, Hooijer GKJ, de Boer OJ, Dijk F, et al. Macrophage-secreted MMP9 induces mesenchymal transition in pancreatic cancer cells via PAR1 activation. Cellular Oncology. 2020; 43(6):1161–74. https://doi.org/10.1007/s13402-020-00549-x PMID: 32809114

123. Sanyal R, Polyak MJ, Zuccolo J, Puri M, Deng L, Roberts L, et al. MS4A4A: a novel cell surface marker for M2 macrophages and plasma cells. Immunology & Cell Biology. 2017; 95(7):611–9. https://doi.org/10.1038/icb.2017.18 PMID: 28303902

124. Wang M, Zhang X, Zhang S, Liu Z. Zebrafish fatty acids receptor Gpr84 enhances macrophage phagocytosis. Fish & Shellfish Immunology. 2019; 84:1098–9. https://doi.org/10.1016/j.fsi.2018.11.023 PMID: 30414894

125. Venkataraman C, Kuo F. The G-protein coupled receptor, GPR84 regulates IL-4 production by T lymphocytes in response to CD3 crosslinking. Immunology Letters. 2005; 101(2):144–53. https://doi.org/10.1016/j.imlet.2005.05.010 PMID: 15993493

126. Liu Q, Zhu F, Liu X, Lu Y, Yao K, Tian N, et al. Non-oxidative pentose phosphate pathway controls regulatory T cell function by integrating metabolism and epigenetics. Nature Metabolism. 2022; 4(5):559–74. https://doi.org/10.1038/s42255-022-00575-z PMID: 35606596

127. Galvan MD, Foreman DB, Zeng E, Tan JC, Bohlson SS. Complement Component C1q Regulates Macrophage Expression of Mer Tyrosine Kinase To Promote Clearance of Apoptotic Cells. The Journal of Immunology. 2012; 188(8):3716–23. https://doi.org/10.4049/jimmunol.1102920 PMID: 22422887

128. Karsunky H, Merad M, Cozzio A, Weissman IL, Manz MG. Flt3 ligand regulates dendritic cell development from Flt3+ lymphoid and myeloid-committed progenitors to Flt3+ dendritic cells in vivo. Journal of Experimental Medicine. 2003; 198(2):305–13. https://doi.org/10.1084/jem.20030323 PMID: 12874263

129. Akbari M, Honma K, Kimura D, Miyakoda M, Kimura K, Matsuyama T, Yui K. IRF4 in dendritic cells inhibits IL-12 production and controls Th1 immune responses against Leishmania major. The Journal of Immunology. 2014; 192(5):2271–9. https://doi.org/10.4049/jimmunol.1301914 PMID: 24489086

130. Nilsson A, Vesterlund L, Oldenborg P-A. Macrophage expression of LRP1, a receptor for apoptotic cells and unopsonized erythrocytes, can be regulated by glucocorticoids. Biochemical and Biophysical Research Communications. 2012; 417(4):1304–9. https://doi.org/10.1016/j.bbrc.2011.12.137 PMID: 22234309

131. Grabher D, Hofer S, Ortner D, Heufler C. In human monocyte derived dendritic cells SOCS1 interacting with CYTIP induces the degradation of CYTIP by the proteasome. PLOS ONE. 2013; 8(2). https://doi.org/10.1371/journal.pone.0057538 PMID: 23469018

132. Ding H, Xu H, Zhang T, Shi C. Identification and validation of M2 macrophage-related genes in endometriosis. Heliyon. 2023; 9(11). https://doi.org/10.1016/j.heliyon.2023.e22258 PMID: 38058639

133. Lei F, Cui N, Zhou C, Chodosh J, Vavvas DG, Paschalis EI. CSF1R inhibition by a small-molecule inhibitor is not microglia specific; affecting hematopoiesis and the function of macrophages. Proceedings of the National Academy of Sciences. 2020; 117(38):23336–8. https://doi.org/10.1073/pnas.1922788117 PMID: 32900927

134. Sehgal A, Irvine KM, Hume DA. Functions of macrophage colony-stimulating factor (CSF1) in development, homeostasis, and tissue repair. Seminars in Immunology. 2021; 54. https://doi.org/10.1016/j.smim.2021.101509 PMID: 34742624

135. Ji L, Guo W. Single-cell RNA sequencing highlights the roles of C1QB and NKG7 in the pancreatic islet immune microenvironment in type 1 diabetes mellitus. Pharmacological Research. 2023; 187. https://doi.org/10.1016/j.phrs.2022.106588 PMID: 36464147

136. Martinez-Campesino L, Kocsy K, Cañedo J, Johnston JM, Moss CE, Johnston SA, et al. Tribbles 3 deficiency promotes atherosclerotic fibrous cap thickening and macrophage-mediated extracellular matrix remodelling. Frontiers in Cardiovascular Medicine. 2022; 9. https://doi.org/10.3389/fcvm.2022.948461 PMID: 36158793